

ACCEPTED VERSION

R. J. Dyson, J. E. F. Green, J. P. Whiteley, H. M. Byrne

An investigation of the influence of extracellular matrix anisotropy and cell-matrix interactions on tissue architecture

Journal of Mathematical Biology, 2016; 72(7):1775-1809

© Springer-Verlag Berlin Heidelberg 2015

The final publication is available at Springer via <http://dx.doi.org/10.1007/s00285-015-0927-7>

PERMISSIONS

<http://www.springer.com/gp/open-access/authors-rights/self-archiving-policy/2124>

Springer is a green publisher, as we allow self-archiving, but most importantly we are fully transparent about your rights.

Publishing in a subscription-based journal

By signing the Copyright Transfer Statement you still retain substantial rights, such as self-archiving:

"Authors may self-archive the author's accepted manuscript of their articles on their own websites. Authors may also deposit this version of the article in any repository, provided it is only made publicly available 12 months after official publication or later. He/ she may not use the publisher's version (the final article), which is posted on SpringerLink and other Springer websites, for the purpose of self-archiving or deposit. Furthermore, the author may only post his/her version provided acknowledgement is given to the original source of publication and a link is inserted to the published article on Springer's website. The link must be provided by inserting the DOI number of the article in the following sentence: "The final publication is available at Springer via [http://dx.doi.org/\[insert DOI\]](http://dx.doi.org/[insert DOI])"."

1 December 2016

<http://hdl.handle.net/2440/94345>

An investigation of the influence of extracellular matrix anisotropy and cell-matrix interactions on tissue architecture

R.J. Dyson · J.E.F. Green · J.P. Whiteley · H.M. Byrne

Received: date / Accepted: date

Abstract Mechanical interactions between cells and the fibrous extracellular matrix (ECM) in which they reside play a key role in tissue development. Mechanical cues from the environment (such as stress, strain and fibre orientation) regulate a range of cell behaviours, including proliferation, differentiation and motility. In turn, the ECM structure is affected by cells exerting forces on the matrix which result in deformation and fibre realignment. In this paper we develop a mathematical model to investigate this mechanical feedback between cells and the ECM. We consider a three-phase mixture of collagen, culture medium and cells, and formulate a system of partial differential equations which represents conservation of mass and momentum for each phase. This modelling framework takes into account the anisotropic mechanical properties

R. J. Dyson¹
School of Mathematics, The Watson Building,
University of Birmingham, Edgbaston,
Birmingham, B15 2TT, UK.
E-mail: R.J.Dyson@bham.ac.uk

J.E.F. Green¹
School of Mathematical Sciences, University of Adelaide,
Adelaide, SA, 5005, Australia.
E-mail: edward.green@adelaide.edu.au

¹ Joint first authors

J.P. Whiteley
Department of Computer Science, University of Oxford,
Wolfson Building, Parks Road, Oxford, OX1 3QD, UK
E-mail: Jonathan.Whiteley@comlab.ox.ac.uk

H.M. Byrne
Department of Computer Science, University of Oxford,
Wolfson Building, Parks Road, Oxford, OX1 3QD, UK; and
Mathematical Institute, University of Oxford,
Andrew Wiles Building, Radcliffe Observatory Quarter
Woodstock Road, Oxford, OX2 6GG, UK.
E-mail: Helen.Byrne@maths.ox.ac.uk

of the collagen gel arising from its fibrous microstructure. We also propose a cell-collagen interaction force which depends upon fibre orientation and collagen density. We use a combination of numerical and analytical techniques to study the influence of cell-ECM interactions on pattern formation in tissues. Our results illustrate the wide range of structures which may be formed, and how those that emerge depend upon the importance of cell-ECM interactions.

Keywords Multiphase model · Collagen fibres · Cell aggregation · Mechanics

1 Introduction

Understanding how tissues grow has long been an important goal of biological research (Thompson, 1942). The normal development, growth and regeneration of biological tissues all require the coordination of cell behaviours such as proliferation, differentiation and migration, dysregulation of these processes being associated with disease states *e.g.* Ingber (2008); Jaalouk and Lammerding (2009); Kumar and Weaver (2009); Soto and Sonnenschein (2004). In the late 19th century, embryologists often focused on the role of mechanics in developmental events (see *e.g.* Thompson (1942)), but the rapid progress in biochemistry and molecular biology in the latter half of the 20th century shifted the emphasis towards understanding patterns of gene expression, and how these might be affected by soluble growth factors and signalling molecules (Ingber, 2006; Soto and Sonnenschein, 2004). Recently there has been renewed interest in tissue mechanics, as experimental results have revealed that mechanical interactions between cells and the extracellular matrix (ECM) in which they reside play an important role in regulating processes such as morphogenesis, tissue regeneration and tumour development (Cukierman and Bassi, 2010; Lopez et al, 2008; Nelson and Bissell, 2006; Strand et al, 2010).

The ECM is a complex material, composed of collagens, elastins, proteoglycans and many other components, its precise composition and organisation varying between tissues (Cukierman and Bassi, 2010; Martins-Green and Bissell, 1995). It provides a scaffold which supports cell adhesion and migration, and thus plays an important role in determining tissue architecture (Bissell and Radisky, 2001; Nelson and Bissell, 2006). It is not, however, a passive structural framework; it influences cell behaviour, sometimes in striking ways. In some cases, specific matrix components may be required to elicit a particular cell response *e.g.* collagen regulates migration of the neural crest cells and normal formation of the neural tube, and also appears to play an important role in angiogenesis (Martins-Green and Bissell, 1995). More generic features of the ECM, including mechanical factors such as its stiffness, the level of stress or strain, or the orientation of fibres within it, can also affect behaviours such as proliferation, differentiation, motility, formation of stress fibres and, in the case of stem cells, their commitment fate (Byfield et al, 2009; Engler et al, 2006; Ingber, 2006; Lopez et al, 2008; Peyton et al, 2007). Furthermore, the ECM can exert its effects on cells indirectly, through interactions with diffusible chemical signals — *e.g.* by binding or altering the transport of growth

factors (Wipff et al, 2007). We note that cell-ECM interactions are often reciprocal. The cells can secrete (or degrade) ECM constituent molecules, and cross-link or re-orient its fibres by exerting forces upon them. Thus the ECM may evolve over time, due to remodelling during development, regeneration following injury, or as a result of disease processes (Cukierman and Bassi, 2010; Martins-Green and Bissell, 1995).

The importance of cell-ECM interactions in tissue development has received particular attention in the context of the mammary gland (both normal development and tumourigenesis) (Kumar and Weaver, 2009; Martins-Green and Bissell, 1995; Ronnov-Jessen and Bissell, 2008; Weigelt and Bissell, 2008), vasculogenesis and angiogenesis (Kirkpatrick et al, 2007; Korff and Augustin, 1999; Manoussaki et al, 1996). For the mammary gland, it has been observed that normal and malignant breast cells are morphologically indistinguishable when grown as monolayers *in vitro*, but when cultured in a three-dimensional, laminin-rich ECM, normal cells stop proliferating and form polarised acinar (spherical) structures, whilst cancer cells continue to proliferate and form disorganised, tumour-like structures (Petersen et al, 1992; Weigelt and Bissell, 2008). In order to study the key physical processes that regulate mammary epithelial cell organisation and behaviour, *in vitro* tissue organogenesis models have been developed which attempt to mimic the three-dimensional *in vivo* matrix environment more closely. In the particular setup used by Dhimolea et al (2010); Krause et al (2008), the breast epithelial cells are seeded into a gel consisting of variable quantities of collagen together with Matrigel and culture medium consisting of nutrient solution and water. The cells organise themselves into small aggregates, forming either acini (spherical structures) or ducts (elongated cylindrical structures). The proportions in which these structures form can be controlled by varying the ECM composition (*i.e.* the relative proportions of collagen, Matrigel and water). The *in vitro* angiogenesis experiments described in Korff and Augustin (1999) and Kirkpatrick et al (2007) are similar, in that endothelial cell aggregates or microvessel fragments respectively, are seeded within a collagen gel. Over a period of days, sprouts form from these initial cell clusters, with the cells appearing to align along the fibres of the collagen matrix. However, mechanical feedback is also observed, whereby forces exerted by the cells realign the fibres.

The examples mentioned above show the potentially significant influences of mechanical interactions between cells and the fibrous ECM on pattern formation *in vitro*. The aim of the current study is to develop a mathematical model that can be used to explore how such interactions might affect tissue architecture. The model presented here investigates the idea that patterns exhibited by the arrangement of cells within the tissue can be generated through mechanical interactions, as a result of cells exerting forces which deform the ECM and thereby alter the fibre alignment. The fibre orientation, in turn, guides cell migration and, hence, affects the spatial distribution of forces exerted on the ECM. A simple schematic illustrating these concepts is shown in Fig. 1. In the absence of a complete set of data on cell-generated forces and ECM mechanical properties, our aim here is to explore qualitative behaviour

in a generic setting, rather than seek quantitative agreement with particular experiments. However, our modelling framework is suitable for specialisation to experiments such as those described in Dhimolea et al (2010); Korff and Augustin (1999) when the appropriate data become available.

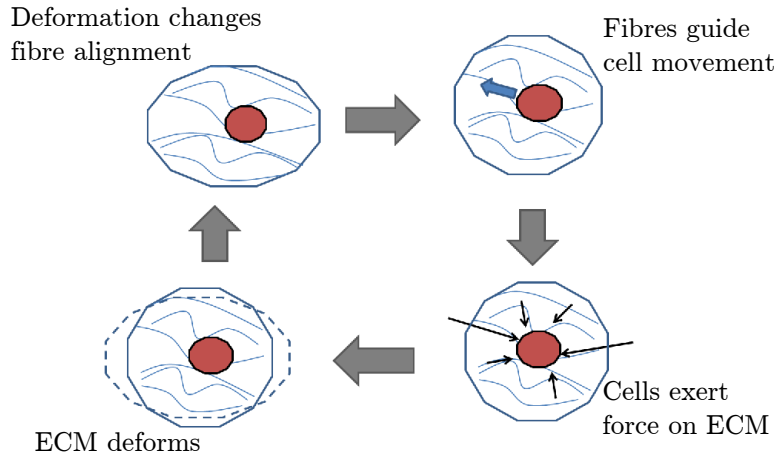


Fig. 1: A schematic diagram illustrating the principles underlying our mathematical model.

A number of previous mathematical models of processes such as morphogenesis, vasculogenesis and wound healing have included the effects cell–ECM interactions (Manoussaki et al, 1996; Murray, 1993; Namy et al, 2004; Oster et al, 1983; Tosin et al, 2006; Tranquillo and Murray, 1993). The earliest of these were the mechanochemical models of Murray and coworkers *e.g.* Oster et al (1983); Tranquillo and Murray (1993). They proposed that cells move by a combination of diffusion and advection with the ECM, with the cell flux being prescribed in terms of the cell density and ECM velocity, whilst the ECM flux is derived from a force balance applied to the whole system. In later models (*e.g.* Tosin et al (2006)), a more detailed approach was employed using mixture theory (Drew, 1983), in which mass and momentum balances are derived for each constituent species. An advantage of this framework is that it is easily extended to include additional cell populations, ECM components, and other species (such as culture medium) (Lemon et al, 2006). Multiphase models require the introduction of constitutive relations to describe the mechanical properties of the different phases. Most models treat the ECM as an isotropic elastic or viscoelastic material, such as a Kelvin-Voigt viscoelastic solid, or Maxwell fluid (Barocas et al, 1995; Tranquillo and Murray, 1993). However, the ECM is often anisotropic (*e.g.* due to the presence of collagen, as described above), and this can have an important effect on cell behaviour.

The mechanical behaviour of fibrous materials is complex, and the subject of intense research (see *e.g.* Petrie (1999) and references therein), motivated by both biological and industrial applications. The mechanics of textile fibres (felt, or tufts of fibres, undergoing elongation or the carding process) have been studied, both experimentally and theoretically by Kabla and Mahadevan (2007); Lee and Ockendon (2005). Similar experimental (Vader et al, 2009), and theoretical (Green and Friedman, 2008), studies of collagen gels have also been undertaken. In biological contexts, however, the focus is frequently on how properties such as fibre alignment or ECM deformation affect cell behaviour. One of the best-studied models to incorporate the feedback between fibre direction and cell migration is the so-called anisotropic biphasic theory (Barocas and Tranquillo, 1997). Here a fibre orientation tensor is introduced, which evolves with the deformation of the ECM and influences cell migration, but does not affect the transmission of stresses through the matrix. Other models account for ECM deposition or degradation, and allow fibre orientation to bias cell movement (*e.g.* Chauviere et al (2007); Hillen (2006); Olsen et al (1999); Painter (2009)), but assume the forces exerted by the cells do not affect fibre orientation.

A more complete theory for cell-ECM interactions, including the mechanics of fibrous ECM was presented by Cook (1995), and applied to the healing of dermal wounds. He considered factors including the nonlinear viscoelastic behaviour of the ECM, and introduced a probability distribution function for the fibre direction, which evolves with the deformation of the material. Similar approaches have been used to understand the rheology of a suspension of fibres in a Newtonian fluid, often motivated by industrial applications (Hinch and Leal, 1975, 1976; Petrie, 1999). However, these models are generally too complicated to be analytically tractable. More recently, simpler anisotropic models have been formulated to describe the behaviour of biological materials such as collagen gels, plant cell walls or suspensions of biomolecules, by treating them as transversely isotropic fluids (Dyson and Jensen, 2010; Green and Friedman, 2008; Holloway et al, 2015). In these models, the stress in the material depends both on the rate of strain and the fibre direction, which is uniquely specified at each point by a unit vector. The fibre alignment can change in space and time due to advection with the flow, but this approach avoids the complication of an evolving probability distribution for the fibre direction. However, until now these models have not been used to study the interplay between anisotropic matrix mechanics and cell-derived forces, and their effect on cell behaviour.

This paper is organised as follows. In §2 we formulate a multiphase model for *in vitro* cells within a fibrous gel such as collagen. In §3, we highlight the effect of matrix anisotropy on cell behaviour by presenting a linearised analysis of a simplified version of the model (assuming that the cells are sparsely-seeded). We then use numerical simulations in §4 to investigate the behaviour of the model when these simplifying assumptions are relaxed. We illustrate the range of qualitatively different patterns which can arise as model parameters are varied. We conclude in §5 with a summary of our main results, and a discussion of possible avenues for future work.

2 Model formulation

We adopt a multiphase modelling framework (Drew, 1983), and consider a three phase mixture, comprising cells, collagen gel and medium (nutrient solution, and/or extracellular water), which occupies a region, \mathcal{R}^* . The volume fractions of the cells, collagen and medium are denoted by $\phi_n(\mathbf{x}, t)$, $\phi_c(\mathbf{x}, t)$ and $\phi_m(\mathbf{x}, t)$, respectively (where \mathbf{x} is a Cartesian position vector and t denotes time). We assume there are no voids, so that

$$\phi_n + \phi_c + \phi_m = 1. \quad (1)$$

For simplicity, we assume that cell proliferation and death are negligible and, similarly, that collagen is neither produced nor degraded. Cells, collagen and medium are assumed to have constant density and we can thus cancel this factor from the mass balance equations. Denoting the velocities of the cells, collagen and medium by $\mathbf{v}_n(\mathbf{x}, t)$, $\mathbf{v}_c(\mathbf{x}, t)$ and $\mathbf{v}_m(\mathbf{x}, t)$, respectively, conservation of mass then gives

$$\frac{\partial \phi_n}{\partial t} + \nabla \cdot (\phi_n \mathbf{v}_n) = 0, \quad (2a)$$

$$\frac{\partial \phi_c}{\partial t} + \nabla \cdot (\phi_c \mathbf{v}_c) = 0, \quad (2b)$$

$$\frac{\partial \phi_m}{\partial t} + \nabla \cdot (\phi_m \mathbf{v}_m) = 0. \quad (2c)$$

We denote by $\boldsymbol{\sigma}_n$, $\boldsymbol{\sigma}_c$ and $\boldsymbol{\sigma}_m$ the stress tensors for the cells, collagen and medium. Neglecting inertial effects, the momentum balance in each phase is given by:

$$\nabla \cdot (\phi_n \boldsymbol{\sigma}_n) + \mathbf{k}_{cn} \cdot (\mathbf{v}_c - \mathbf{v}_n) - k_{mn}(\mathbf{v}_n - \mathbf{v}_m) - \mathbf{F}_c + p \nabla \phi_n = \mathbf{0}, \quad (3a)$$

$$\nabla \cdot (\phi_c \boldsymbol{\sigma}_c) - \mathbf{k}_{cn} \cdot (\mathbf{v}_c - \mathbf{v}_n) - \mathbf{k}_{cm} \cdot (\mathbf{v}_c - \mathbf{v}_m) + \mathbf{F}_c + p \nabla \phi_c = \mathbf{0}, \quad (3b)$$

$$\nabla \cdot (\phi_m \boldsymbol{\sigma}_m) + \mathbf{k}_{cm} \cdot (\mathbf{v}_c - \mathbf{v}_m) + k_{mn}(\mathbf{v}_n - \mathbf{v}_m) + p \nabla \phi_m = \mathbf{0}, \quad (3c)$$

where p is a pressure common to all phases, and \mathbf{k}_{cn} , \mathbf{k}_{cm} and k_{mn} are the interphase drag coefficients. We allow \mathbf{k}_{cn} and \mathbf{k}_{cm} to be rank two tensors, as we assume the drag between the collagen and other phases may depend upon the fibre orientation. In equations (3a)-(3b), we denote by \mathbf{F}_c the force that the cells exert on the ECM as they adhere to and pull upon it. For simplicity, we assume that these cell-derived forces are transmitted to the fibrous collagen network and, thus, neglect forces exerted by cells on the medium.

We also require an equation for the evolution of the fibre direction, which we denote by a unit vector, $\mathbf{a}(\mathbf{x}, t)$. We assume fibres are advected with the flow of the collagen, so

$$\frac{\partial \mathbf{a}}{\partial t} + (\mathbf{v}_c \cdot \nabla) \mathbf{a} + \mathbf{a} \cdot [(\mathbf{a} \cdot \nabla) \mathbf{v}_c] \mathbf{a} = (\mathbf{a} \cdot \nabla) \mathbf{v}_c, \quad (4)$$

(see Dyson and Jensen (2010); Green and Friedman (2008); Holloway et al (2015) for a derivation). Here the first terms represent the advection of fibres, the final term on the left hand side allows for stretching of the fibres and the term on the right hand side represents reorientation by the flow. Equation (4) is a special case of an equation derived by Ericksen (1960), and is appropriate for fibres for which the ratio of their thickness to their length tends to zero.

Our model thus consists of equations (1)-(4) for the volume fractions and velocities of the cells, collagen and medium, and the alignment of the collagen fibres. We remark that in mixture theory all field variables are either volume-averaged (*e.g.* velocities) or functions of averaged quantities (*e.g.* stresses). This applies to the fibre alignment vector, \mathbf{a} , which should be viewed as an averaged quantity. In order to close the model, in the next section we introduce constitutive relations which specify the functional forms of the stress tensors, drag coefficients and the cell-collagen interaction force, before giving appropriate initial and boundary conditions in §2.2.

2.1 Constitutive relations

2.1.1 The stress tensors ($\boldsymbol{\sigma}_n$, $\boldsymbol{\sigma}_c$ and $\boldsymbol{\sigma}_m$)

Following O’Dea et al (2008), the cells are modelled as an incompressible viscous fluid, with

$$\sigma_{n_{ij}} = -p_n \delta_{ij} + 2\mu_n^* e_{n_{ij}} + \left(\kappa_n^* - \frac{2}{3}\mu_n^* \right) e_{n_{kk}} \delta_{ij}, \quad (5)$$

where p_n is the cell pressure, μ_n^* and κ_n^* are the shear and bulk viscosities of the cells, and $e_{n_{ij}}$ is their rate of strain tensor, given by

$$e_{n_{ij}} = \frac{1}{2} \left(\frac{\partial v_{n_i}}{\partial x_j} + \frac{\partial v_{n_j}}{\partial x_i} \right).$$

The cell pressure, p_n , is assumed to comprise the pressure, p , which is common to all phases (see equation (3)), and an additional, prescribed, intraphase pressure, $\Sigma_n(\phi_n)$, caused by cell-cell interactions, so that

$$p_n = p + \Sigma_n(\phi_n). \quad (6)$$

We anticipate cell-cell attraction when the cell density is low and cell-cell repulsion due to overcrowding when it is high. Thus, following Breward et al (2002); Green et al (2009), we set

$$\Sigma_n(\phi_n) = \Gamma^* \frac{\phi_n - \Phi}{(1 - \phi_n)^2}, \quad (7)$$

where the tension constant Γ^* describes the cells’ affinity for the close-packing density, Φ (where $0 < \Phi < 1$). In practice the function $\Sigma_n(\phi_n)$ enters equation (3a) via the combination $\phi_n \Sigma_n$, and a graph of this function is plotted in

Fig. 2 (for the case $\Gamma^* = 1$, $\Phi = 0.8$). Its only turning point occurs at $\phi_n = \phi_n^* = \Phi/(2 - \Phi)$: for $\phi_n < \phi_n^*$, cells are driven up gradients of cell density (corresponding to cell-cell attraction), whilst for $\phi_n > \phi_n^*$ the effect is repulsive.

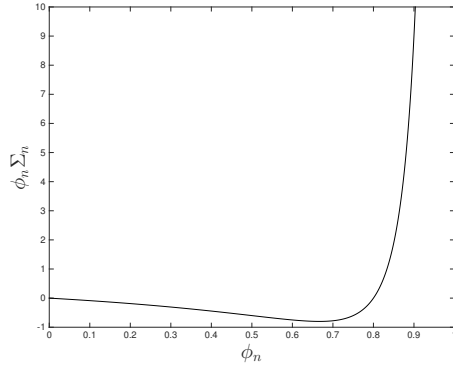


Fig. 2: A plot of the function $\phi_n \Sigma_n(\phi_n)$ (see equation (7)) for $\Gamma^* = 1$ and $\Phi = 0.8$ (so that $\phi_n^* = 2/3$). This demonstrates the functional dependence of (3a) on Σ_m

The structure of collagen gels is complex, which makes modelling their mechanical properties difficult. However, experimental studies suggest that they can be treated as isotropic, upper-convected Maxwell fluids (Barocas et al, 1995; Knapp et al, 1997; Schreiber et al, 2003). In what follows, we treat the gel as a viscous fluid, justifying this simplifying assumption by estimating its Deborah number to be small (the Deborah number is the ratio of the stress relaxation timescale to the experimental timescale). Schreiber et al (2003) report values of the shear modulus (G^*) and viscosity (μ^*) of collagen gels to be $G^* = 1.185 \times 10^4$ dyne cm^{-2} and $\mu^* = 1.24 \times 10^8$ dyne s cm^{-2} . Given a timescale T^* for pattern formation of several days ($10^5 - 10^6$ s), we estimate of the Deborah number to be $\mathcal{D} = \mu^*/G^*T^* \sim 0.01 - 0.1$. We conclude that it is reasonable to treat the gel as a viscous fluid. We note, however, that gel preparation methods vary between groups, and so it is possible that elastic effects may contribute to experimental results such as those of Dhimolea et al (2010); Korff and Augustin (1999). We postpone consideration of such effects to later work.

While the studies of collagen gel mechanics cited above neglect fibre orientation and assume the gel is isotropic, we assume that the collagen's fibrous microstructure plays an important role in determining tissue architecture. Following Dyson and Jensen (2010); Green and Friedman (2008); Holloway et al (2015), we view the collagen as an incompressible, transversely isotropic viscous fluid, having a single preferred direction defined by the fibre alignment

at each point in the material. Accordingly, we assume that

$$\begin{aligned} \sigma_{c_{ij}} = & -p\delta_{ij} + 2\mu_c^* e_{c_{ij}} + \left(\kappa_c^* - \frac{2}{3}\mu_c^* \right) e_{c_{kk}} \delta_{ij} + \mu_1^* a_i a_j + \mu_2^* a_i a_j a_k a_l e_{c_{kl}} \\ & + 2\mu_3^* (a_i a_l e_{c_{jl}} + a_j a_m e_{c_{mi}}) + \mu_4^* (a_i a_j e_{c_{kk}} + \delta_{ij} a_l a_m e_{c_{lm}}) \end{aligned} \quad (8)$$

where $\mathbf{a}(\mathbf{x}, t) = (a_i)$ is the fibre direction, and $e_{c_{ij}}$ is the rate-of-strain for the collagen. In equation (8), μ_c^* is the isotropic component of the viscosity (*i.e.* the matrix viscosity modified for the presence of the fibres; see Dyson and Jensen (2010); Holloway et al (2015) for details). Similarly, κ_c^* is the isotropic component of the bulk viscosity. The constant μ_1^* represents tension in the fibre direction, so that there is a stress in the fibre direction even when the strain rate is zero. The constant μ_2^* is related to the extensional viscosity in the fibre direction, such that $\mu_2^* + 4\mu_3^*$ gives the enhanced resistance to stretching the material in the fibre direction as opposed to perpendicular to the fibres. The constant μ_3^* is related to the shear viscosity in the fibre direction, such that μ_3^* gives the enhanced resistance to shearing the material in the fibre direction rather than perpendicular to the fibres. Finally, μ_4^* is the anisotropic component of the bulk viscosity. We note that, compared to the constitutive relations presented in Dyson and Jensen (2010); Ericksen (1960); Green and Friedman (2008); Holloway et al (2015), equation (8) contains additional terms involving $e_{c_{kk}}$; such terms are needed because the volume fraction of collagen may vary in time, and hence the velocity field, \mathbf{v}_c , is not solenoidal. A similar functional form, omitting the pressure term, was used in a model of fibre carding (Lee, 2001; Lee and Ockendon, 2005).

To the best of our knowledge, there are no experimental data on typical values of the μ_i^* ($i = 1, 2, 3, 4$) for gels commonly used in cell culture. However, it is well known from studies of fibre suspensions that their response to shear and extension is influenced by the fibre orientation (*e.g.* Petrie (1999)), suggesting that the terms involving μ_2^* and μ_3^* are likely to be important. Similarly, other experimental studies (*e.g.* Takakuda and Miyairi (1996)) have suggested that the collagen fibres may experience tension in particular experimental setups, an effect represented by the term involving μ_1^* in our model.

We model the medium as an isotropic incompressible viscous fluid, with shear and bulk viscosities μ_m^* and κ_m^* respectively, so that

$$\sigma_{m_{ij}} = -p\delta_{ij} + 2\mu_m^* e_{m_{ij}} + \left(\kappa_m^* - \frac{2}{3}\mu_m^* \right) e_{m_{kk}} \delta_{ij} \quad (9)$$

where $e_{m_{ij}}$ is the rate-of-strain tensor for the medium.

2.1.2 The interphase drag terms (k_{mn} , \mathbf{k}_{cn} and \mathbf{k}_{cm})

When prescribing the interphase drag terms we assume that there is no drag if either of the interacting species is absent. Therefore the drag is proportional

to the product of the relevant volume fractions. In the case of cell-medium drag, since both phases are isotropic, we follow Breward et al (2002) and set

$$k_{mn} = D_{mn}^* \phi_n \phi_m, \quad (10a)$$

for some constant $D_{mn}^* \geq 0$.

We assume that the magnitude of cell-collagen and medium-collagen drag depends on the direction of relative motion compared to the fibre orientation. For example, if relative motion between cells and collagen occurs along the fibre direction, \mathbf{a} , the effective drag coefficient is assumed to be $\phi_c \phi_n D_{cn}^*$. However, relative motion normal to the fibre direction is assumed to encounter greater resistance, with the effective drag coefficient being $\phi_c \phi_n (D_{cn}^* + d_{cn}^*)$. We make similar assumptions for the collagen-medium drag. Hence, the drag tensors \mathbf{k}_{cn} and \mathbf{k}_{cm} are given by

$$k_{cni_j} = \phi_c \phi_n [(D_{cn}^* + d_{cn}^*) \delta_{ij} - d_{cn}^* a_i a_j], \quad (10b)$$

$$k_{cm_{ij}} = \phi_c \phi_m [(D_{cm}^* + d_{cm}^*) \delta_{ij} - d_{cm}^* a_i a_j], \quad (10c)$$

where $D_{cn}^* \geq 0$ and $D_{cm}^* \geq 0$ represent the strengths of the drag in the direction parallel to the fibres, and $d_{cn}^* \geq 0$ and $d_{cm}^* \geq 0$ the additional drag contributions in the direction normal to the fibres.

2.1.3 The cell force function (\mathbf{F}_c)

We suppose that the force, \mathbf{F}_c , that the cells exert on the collagen at a point \mathbf{x} is the sum of the forces exerted by cells at surrounding points \mathbf{x}' (where \mathbf{x} is within the ‘sphere of influence’ Ω of the cell at \mathbf{x}' of radius η). The force acts in the direction $(\mathbf{x}' - \mathbf{x})$, and is weighted by distance so that nearby cells have a greater effect. We further assume that the force depends upon the direction of the fibre, with forces being transmitted more effectively along the fibres than through the surrounding material. We hence assume that \mathbf{F}_c has functional form

$$\mathbf{F}_c(\mathbf{x}) = \int_{\Omega} \phi_n(\mathbf{x}') G \left(\frac{\phi_c(\mathbf{x}') \mathbf{a}(\mathbf{x}') \cdot (\mathbf{x} - \mathbf{x}')}{|\mathbf{x} - \mathbf{x}'|} \right) F \left(\frac{|\mathbf{x} - \mathbf{x}'|}{\eta} \right) (\mathbf{x}' - \mathbf{x}) d^N x', \quad (11)$$

where N is the dimension of Ω . In equation (11), the function F describes how the force depends upon the distance between the point \mathbf{x} and a cell at position \mathbf{x}' . The function G represents the extent to which forces are transmitted more effectively along fibres than through non-fibrous matrix material and, therefore, depends upon the volume fraction of collagen fibres, ϕ_c , at the cell’s location, as well as the fibre direction. When the unit vector in the direction of the force exerted by the cell $([\mathbf{x}' - \mathbf{x}]/|\mathbf{x}' - \mathbf{x}|)$ is aligned with the fibre direction at the cell’s location ($\mathbf{a}(\mathbf{x}')$), we assume that the magnitude of the force is maximised. By contrast, setting $G \equiv 1$ would imply that the fibres

are no more effective than the surrounding material at transmitting the force. Henceforth, we fix

$$G = (\phi_c(\mathbf{x}'))^2 \left[\frac{\mathbf{a}(\mathbf{x}') \cdot (\mathbf{x} - \mathbf{x}')}{|\mathbf{x} - \mathbf{x}'|} \right]^2, \quad (12)$$

any constant factors being absorbed into F . This quadratic form is chosen as it is the simplest non-trivial function which is invariant under the transformation $\mathbf{a} \rightarrow -\mathbf{a}$.

Additional assumptions are needed to specify the function F in equation (11). Microscopic analysis of cells in compacting collagen gels suggests that cells exert forces mainly on the small region of gel surrounding them (Stevenson et al, 2010). We assume that the cells exert forces on the collagen in a small ‘ N -sphere’ (*i.e.* a circle in two dimensions, or sphere in three dimensions) of radius $\eta \ll 1$ around them. We can then simplify the integrand in equation (13) by extending the method introduced in (Green et al, 2013). If we write

$$\mathbf{x}' = \mathbf{x} + \eta \boldsymbol{\xi},$$

then $|\boldsymbol{\xi}| = 1$ defines the boundary of the sphere of influence centred at \mathbf{x} , and (11) becomes

$$\mathbf{F}_c(\mathbf{x}) = \eta^{N+1} \int_{\Omega} (\phi_c(\mathbf{x}'))^2 \left(\frac{\mathbf{a}(\mathbf{x}') \cdot \boldsymbol{\xi}}{|\boldsymbol{\xi}|} \right)^2 F(|\boldsymbol{\xi}|) \phi_n(\mathbf{x}') \boldsymbol{\xi} d^N \boldsymbol{\xi}. \quad (13)$$

We exploit the assumption that $\eta \ll 1$ by expanding $\phi_n(\mathbf{x}')$, $\phi_c(\mathbf{x}')$ and $\mathbf{a}(\mathbf{x}')$ as power series in η , substituting the expansions into equation (13), and integrating term by term (for details of this calculation see Appendix A). In this way we find that the cell force is given by

$$\mathbf{F}_c(\mathbf{x}) = 2\lambda \left[(\mathbf{a} \cdot \nabla) (\phi_n \phi_c^2 \mathbf{a}) + \phi_n \phi_c^2 \mathbf{a} (\nabla \cdot \mathbf{a}) + \frac{1}{2} \nabla (\phi_c^2 \phi_n) \right] + O(\eta), \quad (14)$$

where

$$\lambda = \frac{\eta^{N+2}}{N(N+2)} \int_{\Omega} F(|\boldsymbol{\xi}|) |\boldsymbol{\xi}|^2 d^N \boldsymbol{\xi},$$

and we assume $\lambda = O(1)$.

2.2 Initial and boundary conditions

Our model comprises equations (1)-(4), together with the constitutive relations (5)-(10) and (14), which must be solved subject to suitable initial and boundary conditions. We consider a two-dimensional rectangular region, $0 \leq x \leq L_x^*$, $0 \leq y \leq L_y^*$, as this is the simplest in which the effects of anisotropy can become manifest. It is important to note that this is distinct from a 2D biological monolayer culture; here the cells grow in a 3D gel but are constrained to move in one plane only.

We prescribe the initial distributions of cells, collagen and medium,

$$\phi_n(\mathbf{x}, 0) = \phi_{n_0}(\mathbf{x}), \quad \phi_c(\mathbf{x}, 0) = \phi_{c_0}(\mathbf{x}), \quad \phi_m(\mathbf{x}, 0) = \phi_{m_0}(\mathbf{x}) = (1 - \phi_{n_0}(\mathbf{x}) - \phi_{c_0}(\mathbf{x})) \quad (15a)$$

(subject to the constraint (1)). We also specify the initial orientation of the fibres

$$\mathbf{a}(\mathbf{x}, 0) = \mathbf{a}_0(\mathbf{x}). \quad (15b)$$

We assume that the domain is periodic in both x and y . Hence, the boundary conditions are

$$\phi_\alpha(0, y, t) = \phi_\alpha(L_x^*, y, t), \quad \phi_\alpha(x, 0, t) = \phi_\alpha(x, L_y^*, t), \quad (16a)$$

$$\mathbf{v}_\alpha(0, y, t) = \mathbf{v}_\alpha(L_x^*, y, t), \quad \mathbf{v}_\alpha(x, 0, t) = \mathbf{v}_\alpha(x, L_y^*, t), \quad (16b)$$

for $\alpha = n, c, m$.

2.3 Dimensionless equations

The governing equations are nondimensionalised as follows (where tildes indicate dimensionless quantities):

$$(x, y) = L_x^*(\tilde{x}, \tilde{y}), \quad t = T^*\tilde{t}, \quad p = \frac{\mu_c^*}{T^*}\tilde{p}, \quad (\mathbf{v}_n, \mathbf{v}_m, \mathbf{v}_c) = \frac{L_x^*}{T^*}(\tilde{\mathbf{v}}_n, \tilde{\mathbf{v}}_m, \tilde{\mathbf{v}}_c),$$

$$(\boldsymbol{\sigma}_n, \boldsymbol{\sigma}_c, \boldsymbol{\sigma}_m) = \frac{1}{T^*}(\mu_c^*\tilde{\boldsymbol{\sigma}}_n, \mu_c^*\tilde{\boldsymbol{\sigma}}_c, \mu_c^*\tilde{\boldsymbol{\sigma}}_m), \quad \mathbf{F}_c = \frac{\mu_c^*}{L_x^*T^*}\tilde{\mathbf{F}}_c,$$

where the timescale T^* remains to be determined.

The form of equations (1), (2) and (4) is unchanged by this transformation. On substituting for the drag terms, the momentum equations transform to give

$$\begin{aligned} \frac{\partial}{\partial x_j}(\phi_n \sigma_{n_{ij}}) + \phi_c \phi_n [(D_{cn} + d_{cn})\delta_{ij} - d_{cn} a_i a_j] (v_{c_j} - v_{n_j}) \\ - D_{mn} \phi_n \phi_m (v_{n_j} - v_{m_j}) - F_{c_i} + p \frac{\partial \phi_n}{\partial x_i} = 0, \end{aligned} \quad (17a)$$

$$\begin{aligned} \frac{\partial}{\partial x_j}(\phi_c \sigma_{c_{ij}}) - \phi_c \phi_n [(D_{cn} + d_{cn})\delta_{ij} - d_{cn} a_i a_j] (v_{c_j} - v_{n_j}) \\ - \phi_c \phi_n [(D_{cm} + d_{cm})\delta_{ij} - d_{cm} a_i a_j] (v_{c_j} - v_{m_j}) + F_{c_i} + p \frac{\partial \phi_c}{\partial x_i} = 0, \end{aligned} \quad (17b)$$

$$\begin{aligned} \frac{\partial}{\partial x_j}(\phi_m \sigma_{m_{ij}}) + \phi_c \phi_n [(D_{cm} + d_{cm})\delta_{ij} - d_{cm} a_i a_j] (v_{c_j} - v_{m_j}) \\ + D_{mn} \phi_n \phi_m (v_{n_j} - v_{m_j}) + p \frac{\partial \phi_n}{\partial x_i} = 0, \end{aligned} \quad (17c)$$

where we have introduced the dimensionless drag coefficients

$$D_{cn} = \frac{D_{cn}^* L_x^{*2}}{\mu_c^*}, \quad d_{cn} = \frac{d_{cn}^* L_x^{*2}}{\mu_c^*}, \quad D_{cm} = \frac{D_{cm}^* L_x^{*2}}{\mu_c^*}, \quad d_{cm} = \frac{d_{cm}^* L_x^{*2}}{\mu_c^*}, \quad D_{mn} = \frac{D_{mn}^* L_x^{*2}}{\mu_c^*}.$$

Note that in equation (17), and henceforth, the summation convention is used and we tildes are omitted for notational convenience.

The dimensionless forms of the stress tensors and force term are given by

$$\sigma_{n_{ij}} = - \left(p + \Gamma \frac{\phi_n - \Phi}{(1 - \phi_n)^2} \right) \delta_{ij} + 2\beta_n e_{n_{ij}} + \left(\kappa_n - \frac{2}{3}\beta_n \right) e_{n_{kk}}, \quad (18a)$$

$$\begin{aligned} \sigma_{c_{ij}} = & -p\delta_{ij} + 2e_{c_{ij}} + \left(\kappa_c - \frac{2}{3} \right) e_{c_{kk}} \delta_{ij} + \mu_1 a_i a_j + \mu_2 a_i a_j a_k a_l e_{c_{kl}} \\ & + 2\mu_3 (a_i a_l e_{c_{jl}} + a_j a_m e_{c_{mi}}) + \mu_4 (a_i a_j e_{c_{kk}} + \delta_{ij} a_l a_m e_{c_{lm}}), \end{aligned} \quad (18b)$$

$$\sigma_{m_{ij}} = -p\delta_{ij} + 2\beta_m e_{m_{ij}} + \left(\kappa_m - \frac{2}{3}\beta_m \right) e_{m_{kk}} \delta_{ij}, \quad (18c)$$

$$F_{c_i} = 2\Lambda \left(a_j \frac{\partial}{\partial x_j} (\phi_n \phi_c^2 a_i) + \phi_n \phi_c^2 a_i \frac{\partial a_j}{\partial x_j} + \frac{1}{2} \frac{\partial}{\partial x_i} (\phi_c^2 \phi_n) \right), \quad (18d)$$

where we have introduced the dimensionless parameters

$$\begin{aligned} \Gamma = \frac{\Gamma^* T^*}{\mu_c^*}, \quad \kappa_n = \frac{\kappa_n^*}{\mu_c^*}, \quad \kappa_c = \frac{\kappa_c^*}{\mu_c^*}, \quad \kappa_m = \frac{\kappa_m^*}{\mu_c^*}, \quad \beta_n = \frac{\mu_n^*}{\mu_c^*}, \quad \beta_m = \frac{\mu_m^*}{\mu_c^*}, \quad \Lambda = \frac{\lambda T^*}{\mu_c^*}, \\ \mu_1 = \frac{\mu_1^* T^*}{\mu_c^*}, \quad \mu_2 = \frac{\mu_2^*}{\mu_c^*}, \quad \mu_3 = \frac{\mu_3^*}{\mu_c^*}, \quad \mu_4 = \frac{\mu_4^*}{\mu_c^*}, \end{aligned}$$

The parameters κ_α (where, again, $\alpha = n, c, m$) are the ratios of the bulk viscosities of the three phases to the isotropic component of viscosity for the collagen phase, whilst the μ_α are the ratios of the anisotropic terms to the isotropic component of viscosity for the collagen. Natural choices for the timescale of interest are either μ_c^*/Γ^* , the timescale for the cell's self-induced movement (and thus $\Gamma = 1$), or μ_c^*/λ , the timescale over which the force exerted by the cell is transmitted to the collagen (and thus $\Lambda = 1$). Without loss of generality, we make the latter choice.

The initial conditions are mapped to the transformed domain $0 \leq x \leq 1$, $0 \leq y \leq L$, where $L = L_y^*/L_x^*$. Under this transformation the periodic boundary conditions become, for $\alpha = c, m, n$,

$$\phi_\alpha(0, y, t) = \phi_\alpha(1, y, t), \quad \phi_\alpha(x, 0, t) = \phi_\alpha(x, L, t), \quad (19a)$$

$$\mathbf{v}_\alpha(0, y, t) = \mathbf{v}_\alpha(1, y, t), \quad \mathbf{v}_\alpha(x, 0, t) = \mathbf{v}_\alpha(x, L, t). \quad (19b)$$

3 Linearised analysis for sparsely-seeded cells

Our model comprises a system of coupled nonlinear PDEs which must be solved in at least two dimensions to account for the effects of anisotropy. In this section we simplify the model by assuming that the cells are seeded sparsely in the matrix so that, at least for short times, the cell volume fraction will be small. We introduce a small parameter, $\epsilon \ll 1$, which represents a typical value of the (small) cell volume fraction. In addition, we neglect cell viscosity (so $\beta_n = 0$) and the anisotropic components of the drag coefficients, so that $d_{cn} = d_{cm} = 0$ in equations (10). We expand all dependent variables as regular power series in ϵ so that

$$\phi_n = \phi_n^{(0)} + \epsilon \phi_n^{(1)} + \dots, \quad \text{etc.}$$

Under these assumptions, it is straightforward to show that the leading-order solution to the system described in §2.3 is

$$\phi_n^{(0)} = 0, \quad \phi_c^{(0)} = \phi_{c_0}(\mathbf{x}), \quad \phi_m^{(0)} = \phi_{m_0}(\mathbf{x}) = 1 - \phi_{c_0}(\mathbf{x}), \quad (20)$$

$$\mathbf{v}_m^{(0)} = 0, \quad \mathbf{v}_c^{(0)} = 0, \quad p^{(0)} = 0, \quad (21)$$

$$\mathbf{a}^{(0)} = \mathbf{a}_0(\mathbf{x}), \quad \boldsymbol{\sigma}_c^{(0)} = 0, \quad \boldsymbol{\sigma}_m^{(0)} = 0. \quad (22)$$

Equations for $\phi_n^{(1)}$ and $\mathbf{v}_n^{(0)}$ are obtained by balancing $O(\epsilon)$ terms in the mass and momentum equations for the cells:

$$\frac{\partial \phi_n^{(1)}}{\partial t} + \nabla \cdot (\phi_n^{(1)} \mathbf{v}_n^{(0)}) = 0, \quad (23)$$

$$\Gamma \Phi \nabla \phi_n^{(1)} - (D_{cn} \phi_c^{(0)} + D_{mn} \phi_m^{(0)}) \phi_n^{(1)} \mathbf{v}_n^{(0)} - \mathbf{F}_c^{(1)} = 0, \quad (24)$$

where

$$\mathbf{F}_c^{(1)} = \left(2(\mathbf{a}^{(0)} \cdot \nabla) \left(\phi_n^{(1)} (\phi_c^{(0)})^2 \mathbf{a}^{(0)} \right) + 2\phi_n^{(1)} (\phi_c^{(0)})^2 \mathbf{a}^{(0)} (\nabla \cdot \mathbf{a}^{(0)}) + \nabla \cdot \left((\phi_c^{(0)})^2 \phi_n^{(1)} \right) \right). \quad (25)$$

Combining equations (23) and (24) gives

$$\begin{aligned} \frac{\partial \phi_n^{(1)}}{\partial t} = & \nabla \cdot (\mathcal{D} \cdot \nabla \phi_n^{(1)}) + 2\nabla \cdot \left[\frac{\phi_n^{(1)}}{D_{cn} \phi_c^{(0)} + D_{mn} \phi_m^{(0)}} (\mathbf{a}^{(0)} \cdot \nabla) (\mathbf{a}^{(0)} (\phi_c^{(0)})^2) \right. \\ & \left. + \frac{\phi_n^{(1)} (\phi_c^{(0)})^2}{D_{cn} \phi_c^{(0)} + D_{mn} \phi_m^{(0)}} (\nabla \cdot \mathbf{a}^{(0)}) \mathbf{a}^{(0)} + \frac{\phi_n^{(1)} \phi_c^{(0)}}{D_{cn} \phi_c^{(0)} + D_{mn} \phi_m^{(0)}} \nabla \phi_c^{(0)} \right], \quad (26a) \end{aligned}$$

where the cell dispersion tensor \mathcal{D} has components

$$\mathcal{D}_{ij} = \frac{1}{D_{cn} \phi_c^{(0)} + D_{mn} \phi_m^{(0)}} \left\{ -\Gamma \Phi \delta_{ij} + (\phi_c^{(0)})^2 \delta_{ij} + 2(\phi_c^{(0)})^2 a_i^{(0)} a_j^{(0)} \right\}. \quad (26b)$$

Thus, in the case of sparsely seeded cells, our model reduces to an advection-diffusion equation for cell movement. A novel feature of equation (26a), compared to classical mechanochemical models of tissue development Murray (1993), is that the diffusion is both anisotropic (depending upon the fibre orientations) and nonlinear (depending upon the cell and collagen volume fractions). We further note there is a nonlinear haptotactic term (the final term in square brackets in equation (26a)), which drives cells down, rather than up, gradients of collagen density. This is because \mathbf{F}_c , the force acting on the collagen, is assumed to act in the direction of increasing cell and collagen density (see equation (14)). Consequently, the equal and opposite force acting on the cells will tend to drive them in the opposite direction.

These analytical results provide a useful check on our numerical code for the cases in which the relevant assumptions hold (see §4). It should be noted that for certain parameter values the term involving Φ in \mathcal{D}_{ij} may lead to an ill-posed backward heat equation for $\phi_n^{(1)}$ (see equations (26)), when, as here, cell viscosity is neglected. In such cases, the inclusion of cell viscosity renders the model well posed (Breward et al, 2002; Byrne and Preziosi, 2003; Byrne et al, 2003).

We remark that the evolution of $\phi_n = \epsilon\phi_n^{(1)}$ depends on $\mathbf{a}^{(0)}$ only, *i.e.* the initial fibre configuration. We would need to continue to higher-order terms to determine how the cells influence the fibre orientation. Since the analysis at higher order is involved and the resulting equations not analytically tractable, we choose not to pursue this here.

4 Numerical simulations

In this section we present results generated from numerical simulations of equations (2), (17)-(19). The dimensionless model contains many parameters, and so only a limited investigation is undertaken here, to illustrate the effect that variation of certain parameters has on the system dynamics and the range of qualitative behaviours that the model exhibits.

4.1 Numerical methods

The velocity of each phase and the pressure are calculated by using the finite element method described by (Osborne and Whiteley, 2010). The hyperbolic equations (2) governing mass conservation of each phase are solved by the finite volume method, which is equivalent to a discontinuous Galerkin method with piecewise constant solution on each element (see, for example, Cockburn and Shu (1998)). Equation (4), governing the fibre direction, is solved using the continuous Galerkin finite element method (see, for example, Eriksson et al (1996)). In all simulations, the domain was partitioned into a regular mesh of 80×80 equally sized elements. The code was validated by comparison with the linearised theory presented in §3 (results not shown).

Numerical solutions were computed until either a specified end time was reached, or one of the volume fractions first became zero. In the latter case, our problem becomes a free boundary problem, the boundary delineating the region in which two, rather than three, phases are present. Its solution requires the development of a sophisticated numerical method that can introduce, track, and potentially remove multiple free boundaries. We postpone its development to future work.

We note that if no collagen ($\phi_c \equiv 0$) is present, and the viscosity of the medium is negligible then only cells and medium are present and our model reduces to that of (Green et al, 2009). In this case non-trivial steady states are possible for which regions containing cells at density $\phi_n = \bar{\Phi}$ alternate with regions in which $\phi_n = 0$ (we note that for such cell distributions, the function $\phi_n \Sigma_n \equiv 0$ and, hence, the pressure gradients vanish). When all three phases are present, this non-trivial steady state is not observed. For some of the results presented in §4.2, whilst the numerical simulations appear to reach a state for which the macroscopic features of the solution (*e.g.* size, shape and volume fraction of cell aggregates) do not change, or only change slowly, small-lengthscale fluctuations in the volume fractions appear at later times. We consider these fluctuations to be artifacts of the numerical method, and present results only for times before these effects become apparent. Unfortunately, these artefacts prevent us from making general statements about the existence of steady state solutions of the model.

Whilst it would be desirable to overcome these limitations, we believe our method is sufficiently accurate to illustrate the different types of behaviour our model exhibits. Additionally, for very long times, the effects of cell proliferation and death, ignored here, are likely to become significant.

4.2 Numerical results

Rather than a detailed parameter survey (which is beyond the scope of this paper), we aim to demonstrate the variety of configurations which can be achieved using this model by first considering each effect separately and then in combination. Through appropriate choice of parameter values we will present a variety of qualitatively different cellular patterns including oriented clusters, stripes and networks. We will also demonstrate the impact of feedback from fibres to cells, from cells to fibres and in both directions.

We begin by considering a ‘control’ simulation, against which subsequent simulations will be compared. The parameter values and initial conditions used are given in Table 1; unless otherwise stated these remain fixed. We present heat maps of the volume fractions ϕ_n , ϕ_m and ϕ_c , and a plot of the fibre direction \mathbf{a} , in Figs. 3 and 4 at times $t = 0$ and $t = 4$ respectively. We observe that for this control simulation the cells aggregate, forming two roughly circular clusters, centred on the regions with higher initial cell density. The formation of compact cell clusters, of approximately uniform density with clearly defined edges is similar to the behaviour seen in a one-dimensional

multiphase model of cell aggregation (Green et al, 2009). The collagen density evolves to a similar complementary pattern; with regions of high cell density coinciding with regions of low collagen density. The distribution of the medium follows that of the collagen, both being displaced by cell movement in a similar way (this is unsurprising since, for the control parameter values, both are treated as isotropic fluids of equal viscosity). There is limited realignment of the collagen fibres by cell migration; at long times they curve slightly outwards around the edges of the cell aggregates.

Parameter	Control Value	Initial condition	Control Form
D_{mn}, D_{cn}, D_{cm}	0.1	ϕ_{c0}	$0.5 - 0.005 \sin 2\pi x \sin \frac{2\pi y}{L}$
d_{cn}, d_{cm}	0	ϕ_{m0}	$0.25 - 0.005 \sin 2\pi x \sin \frac{2\pi y}{L}$
β_m, β_n	1	ϕ_{n0}	$0.25 + 0.01 \sin 2\pi x \sin \frac{2\pi y}{L}$
$\mu_1, \mu_2, \mu_3, \mu_4$	0	\mathbf{a}_0	$(1, 0)^T$
Λ	1		
Γ	10		
Φ	0.8		
$\kappa_c, \kappa_m, \kappa_n$	0		
L	1		

Table 1: The control parameters and initial conditions.

We now investigate the effects of fibre alignment on the system's evolution, by setting the initial fibre angle to be $\pi/4$ - *i.e.* :

$$\mathbf{a}(\mathbf{x}, 0) = \mathbf{a}_0 = \begin{pmatrix} \frac{1}{\sqrt{2}} \\ \frac{1}{\sqrt{2}} \end{pmatrix}. \quad (27)$$

By comparing Figs. 4 and 5 it is clear that this change produces a noticeable elongation of the aggregates along the fibre direction. The result is suggestive of a transition from discrete clusters to a more inter-connected structure. For this initial condition the fibres point in the direction parallel to the line connecting the centres of the two regions with initially higher cell density. The change in the initial fibre alignment is equivalent to a variation in the initial volume fraction profiles if the axes were rotated so that the fibre direction aligned with the x -axis.

The initial fibre alignment need not be spatially uniform to observe similar effects. For example, if we adopt the following spatially-varying initial fibre distribution

$$\mathbf{a}(\mathbf{x}, 0) = \mathbf{a}_0 = \begin{pmatrix} \sqrt{1 - 0.25 \sin^2(2\pi x)} \\ 0.5 \sin(2\pi x) \end{pmatrix}, \quad (28)$$

we observe that the aggregates become elongated in the y -direction (see Figs. 6, 7). These case studies are similar to those studied using linearisation in §3, in that the interphase forces and the mechanical properties of the collagen are isotropic; the anisotropic fibre alignment enters the problem through the

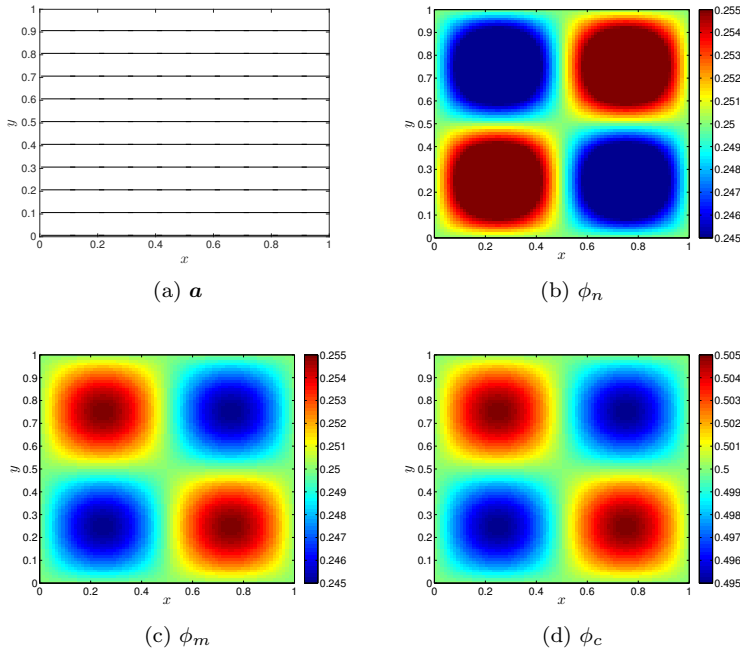


Fig. 3: The initial conditions for the control simulation (see Table 1): (a) fibre alignment, $\mathbf{a}(x, y, 0)$; (b) cell volume fraction, $\phi_n(x, y, 0)$; (c) collagen volume fraction, $\phi_c(x, y, 0)$; (d) medium volume fraction, $\phi_m(x, y, 0)$. Parameter values as given in Table 1. (Note that the colour scale here is exaggerated compared to later figures for ease of visualisation.)

cell force term, \mathbf{F}_c (equation (18d)). Although the cell volume fraction is now $O(1)$ (which violates the assumption made in §3), the simulation results are consistent with those predicted by the analysis, with cells moving preferentially along the fibre direction.

We now consider the effects of varying the model parameters away from their control values. We begin with Γ , the scaled affinity of the cells for the close-packing density; reducing Γ magnifies the effect of the cell-ECM force term, \mathbf{F}_c . The resulting fibre direction and volume fractions, when Γ is decreased from $\Gamma = 10$ (Fig. 4) to $\Gamma = 0.1$ are shown in Fig. 8. The most striking feature is the position of the cell aggregates. In earlier simulations, when aggregates form, they do so in regions where the initial cell density is highest (the bottom left and top right corners). Here, the positioning is reversed. As we can see from the animation (see supplementary material), the cells initially spread out, predominantly in the initial fibre direction, due to the anisotropic cell-ECM force term. As the cells move, collagen is displaced in the opposite direction, creating new regions depleted of collagen in which the cells subsequently form aggregates. These aggregates are not circular, being

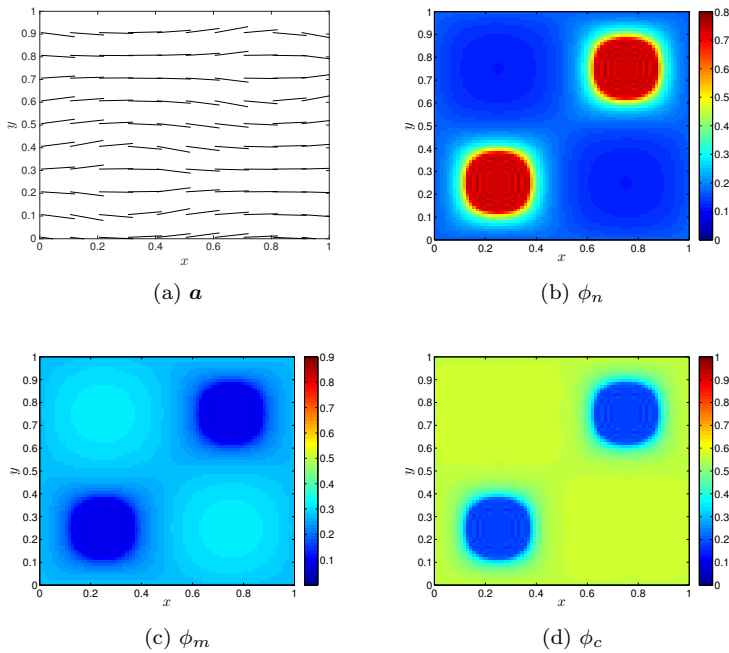


Fig. 4: The control simulation (equations (2), (17)-(19)) at time $t = 4$: (a) fibre alignment, \mathbf{a} ; (b) cell volume fraction, ϕ_n ; (c) medium volume fraction, ϕ_m ; (d) collagen volume fraction, ϕ_c . Parameter values and initial conditions as given in Table 1 and shown in Fig. 3.

slightly compressed in the x -direction due to enhanced cell movement. The realignment of the collagen fibres is particularly pronounced around the edge of the aggregates, while an accumulation of medium is evident at the lateral (but not the upper and lower) edges of the cell clusters.

We now investigate how changing the anisotropic mechanical properties of the collagen influences the system dynamics. Guided by similar multiphase models (see *e.g.* (O’Dea et al, 2008, 2010) and references therein) in which the bulk viscosities are typically taken to be zero, here we set $\kappa_n = \kappa_m = \kappa_c = 0$. Similarly, we set $\mu_4 = 0$, and in this way reduce the dimensions of the parameter space under investigation. Returning to the initial conditions of the control simulation, we look at the effects of varying the parameters μ_1 , μ_2 and μ_3 in turn. When the tension in the fibre direction is large, $\mu_1 = 10$, aggregates that are elongated in the x -direction (*i.e.* the initial fibre direction) form (see Fig. 9). Significant realignment of the fibres also takes place. Whilst the collagen distribution is similar to that seen in earlier simulations, in this case the medium seems to accumulate predominantly at the left- and right-hand edges of the aggregates. To quantify the effect of this parameter on the morphology of the aggregates, we define the anisotropy ratio as follows. We

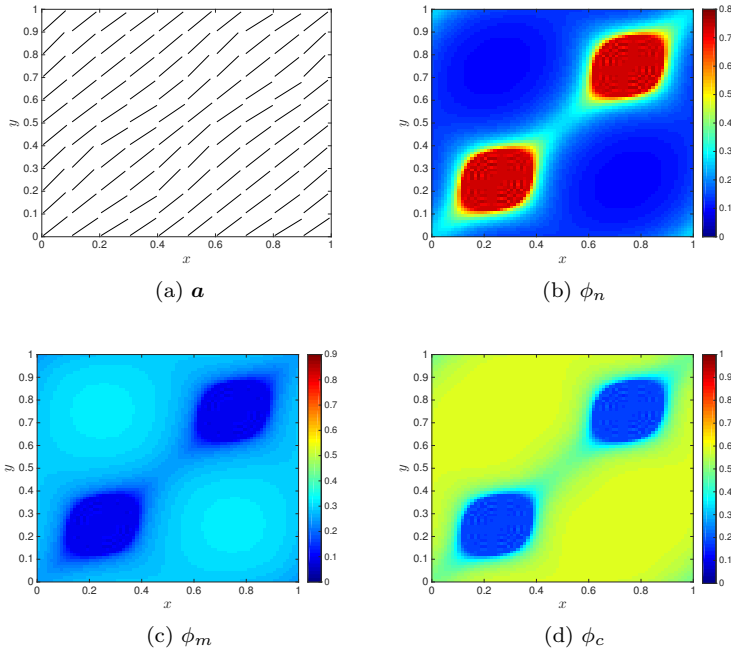


Fig. 5: Simulation results for time $t = 4$ with a diagonal initial fibre alignment (27): (a) fibre alignment, \mathbf{a} ; (b) cell volume fraction, ϕ_n ; (c) medium volume fraction, ϕ_m ; (d) collagen volume fraction, ϕ_c . All other parameter values and initial conditions as in Table 1.

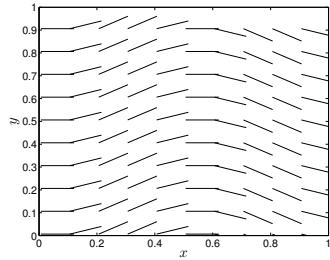


Fig. 6: Spatially varying initial fibre direction, \mathbf{a}_0 defined by equation (28).

first identify the contour $\phi_n = 0.3$ in the distribution of cells. We then define the length in the x -direction, s_x , to be the length of the longest straight line parallel to the x -axis that fits inside the contour. The length in the y -direction, s_y , is defined in an analogous way, and the anisotropy ratio is given by s_y/s_x . Fig. 10 shows how the anisotropy ratio of the resulting cell distribution changes as μ_1 is varied. For small tension in the fibre direction

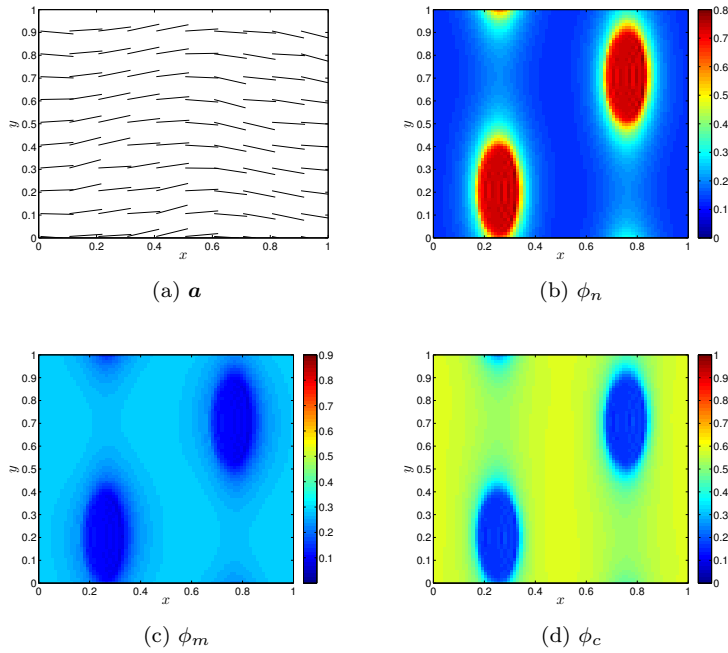


Fig. 7: Simulation results for time $t = 3.2$ with a spatially varying initial fibre alignment as in (28) (see Fig. 6): (a) fibre alignment, \mathbf{a} ; (b) cell volume fraction, ϕ_n ; (c) medium volume fraction, ϕ_m ; (d) collagen volume fraction, ϕ_c . All other parameter values and initial conditions as in Table 1.

relative to the force exerted by the cells on the collagen, (μ_1), we see that the anisotropy ratio is slightly greater than unity, indicating a slight contraction in the x -direction. However as we increase the tension the anisotropy ratio decreases, indicating elongation in the x -direction.

By comparison, setting $\mu_2 = 10$ (recall that μ_2 is related to the extensional viscosity in the fibre direction) has a less pronounced effect (see Fig. 11): the aggregates elongate in the x -direction, but to a lesser degree than in Fig. 9. The medium and collagen distributions are also similar to those seen in the control simulation. Fig. 12 reveals that a more marked effect is seen when $\mu_3 = 10$ (related to the enhancement in shear viscosity in the fibre direction), with the aggregates becoming ellipsoidal (rather than the blunted shapes seen in Fig. 9). The collagen distribution is also markedly different, accumulating in the regions vertically above and below the aggregates, and depleted laterally. When all three of the anisotropic mechanical parameters are nonzero (see *e.g.* Fig. 13 where $\mu_1 = \mu_2 = \mu_3 = 10$), the results most closely resemble the case where only μ_3 was nonzero, which suggests that (at least in this region of parameter space) the contrast in shear viscosity between the direction parallel

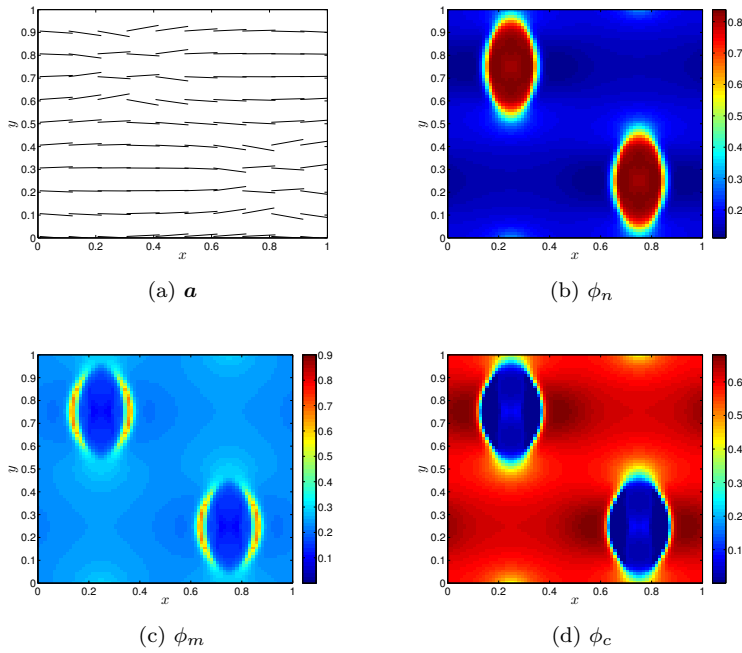


Fig. 8: Simulation results for time $t = 65$ with the scaled affinity of the cells for the close packing density $\Gamma = 0.1$, and all other parameter values and initial conditions as in Table 1. (a) fibre alignment, \mathbf{a} ; (b) cell volume fraction, ϕ_n ; (c) medium volume fraction, ϕ_m ; (d) collagen volume fraction, ϕ_c . (See also supplementary material for animations.)

to the fibres, and that perpendicular to them, has the greatest effect on the morphology of the aggregates.

The effects of initial fibre alignment and anisotropic collagen properties can combine to change the patterns of cell organisation observed. For example, if we take the diagonal initial fibre alignment given by equation (27), and the parameter values used in Fig. 13, the tendency of the two effects to produce elongation of the aggregates in the fibre direction results in the inter-connection of the aggregates, producing a stripe-like pattern (see Fig. 14).

The addition of anisotropic drag can also significantly influence the observed behaviour. Figs. 15 and 16 show simulations taking the initial conditions

$$\phi_{c_0} = 0.25 - 0.15 \sin(2\pi x) \sin(2\pi y), \quad (29a)$$

$$\phi_{m_0} = 0.5, \quad (29b)$$

$$\phi_{n_0} = 0.25 + 0.15 \sin(2\pi x) \sin(2\pi y), \quad (29c)$$

$$\mathbf{a}_0 = (\sqrt{1 - 0.04 \sin^2(2\pi x)}, 0.2 \sin(2\pi x))^T, \quad (29d)$$

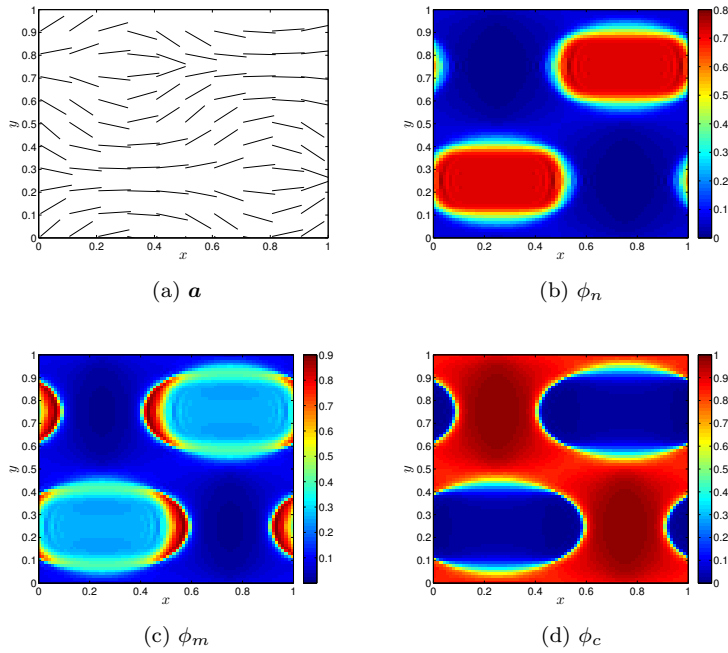


Fig. 9: Simulation results at time $t = 2.2$ with high fibre tension ($\mu_1 = 10$): (a) fibre alignment, \mathbf{a} ; (b) cell volume fraction, ϕ_n ; (c) medium volume fraction, ϕ_m ; (d) collagen volume fraction, ϕ_c . All other parameters and initial conditions as in Table 1.

with the parameter values

$$D_{mn} = D_{cn} = D_{cm} = 0.001, \quad \Phi = 0.5, \quad \Gamma = 0.1 \quad (30)$$

and $d_{cn} = 0$ in Fig. 15 and $d_{cn} = 100$ in Fig. 16. When anisotropic drag is included in Fig. 16, the fibre reorientation by the cells is more pronounced, and we see the formation of a connected network of cells rather than the clusters seen in Fig. 15. In both cases the medium is concentrated between areas which are predominantly either collagen or cells.

Similarly, combining the effects of large fibre tension ($\mu_1 = 10$) and anisotropic drag ($d_{cn} = d_{cm} = 1$) with a spatially varying initial fibre direction as in Eq. (28) can produce a pattern in which stripes of aggregated cells and collagen are aligned in the y direction and separated by thin regions of medium (see Fig. 17).

By additionally varying μ_2 and μ_3 , a new type of qualitative behaviour can be produced. When the fibre tension is small ($\mu_1 = 0.1$), but extensional and shear viscosity in the fibre direction are high ($\mu_2 = \mu_3 = 10$), elliptical cell clusters may form, their major axes being aligned with the local fibre direction (see Fig. 18), which undergoes minimal reorientation. In contrast,

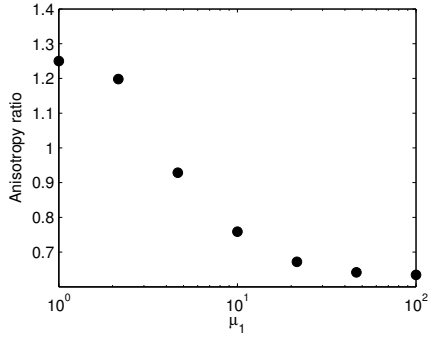


Fig. 10: The anisotropy ratio of the resulting distribution of cells as μ_1 is varied.

when the fibre tension is large ($\mu_1 = 10$; Fig. 19), the cells form aggregates that are elongated in the y -direction and interspersed with strips of medium, whilst the fibre direction significantly remodels to an almost parallel state, aligned perpendicular to the aggregates. Comparing to the behaviour when $\mu_2 = \mu_3 = 0$ (Fig. 17), we observe that this configuration appears to represent a transition between the cluster and stripe patterns.

Our numerical experiments suggest that, in this region of parameter space, varying other model parameters individually (the isotropic drag coefficients D_{cm} , D_{cn} and D_{mn} , and the cell and medium viscosities β_n and β_m) does not significantly alter the long term distribution of cells (results not shown), although the time taken to reach the final configuration may vary. In summary, our results show that a variety of qualitatively different patterns can be formed, depending upon the initial cell and collagen densities, the initial collagen fibre alignment, the anisotropic mechanical properties of the collagen, and the relative affinity of the cells for their close packing density, compared to the cell-ECM force. These patterns include ellipsoidal clusters (*e.g.* Figs. 13 and 18), where the ratios and alignments of the major and minor axes can vary according to the parameter values (*e.g.* Fig. 10), stripes (*e.g.* Figs. 14 and 17) and networks (*e.g.* Fig. 16). We have also examined the feedback from the cells to the collagen fibre orientation (*e.g.* Figs. 9 and 17) and vice versa (*e.g.* Figs. 11- 14). Although our model is generic, rather than focused on any particular experimental system, we note that similar patterns have been generated in *in vitro* experiments *e.g.* (Dhimolea et al, 2010).

5 Discussion

We have developed a new multiphase modelling framework to explore the role of matrix anisotropy in the development of pattern and form in tissues. Whilst some recent models account for ECM fibres directing cell movement

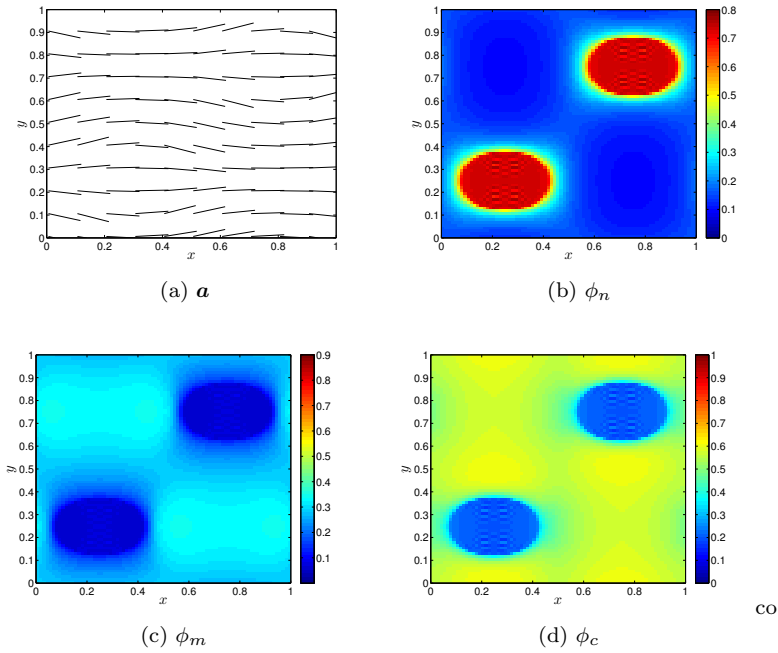


Fig. 11: Simulation results at time $t = 4.7$ with high extensional viscosity in the fibre direction ($\mu_2 = 10$): (a) fibre alignment, \mathbf{a} ; (b) cell volume fraction, ϕ_n ; (c) medium volume fraction, ϕ_m ; (d) collagen volume fraction, ϕ_c . All other parameters and initial conditions as in Table 1.

e.g. Hillen (2006); Painter (2009), they typically neglect the associated mechanical changes, whilst others account for both cell guidance by fibres, and mechanical interactions between the ECM and the cells, but they assume that the fibres have no effect on the mechanical properties of the matrix, which is treated as isotropic (*e.g.* Barocas and Tranquillo (1997); Häcker (2012)). In contrast, our framework allows fibres embedded within the ECM to affect both the collagen mechanics (through the transversely isotropic form of the stress tensor) and cell-ECM interactions (though the anisotropic drag and cell-ECM force terms). The cell-ECM force is modelled via a convolution integral term, an approach which is increasingly being used to represent cell-cell and cell-ECM interactions in continuum models (Gerisch and Chaplain, 2008; Green et al, 2010; Szymanska et al, 2009). For an isotropic ECM, recent work (Green et al, 2013) has shown that, if the ‘sphere of influence’ of each cell is small, the nonlocal term can be approximated by the gradient of a function of cell and ECM density. This representation of the force term is similar to that used in the mechanochemical theory developed by Murray and coworkers (Murray, 1993). Here, we have used a similar argument to show that when the force depends on the fibre direction, it can be reduced to a form which includes

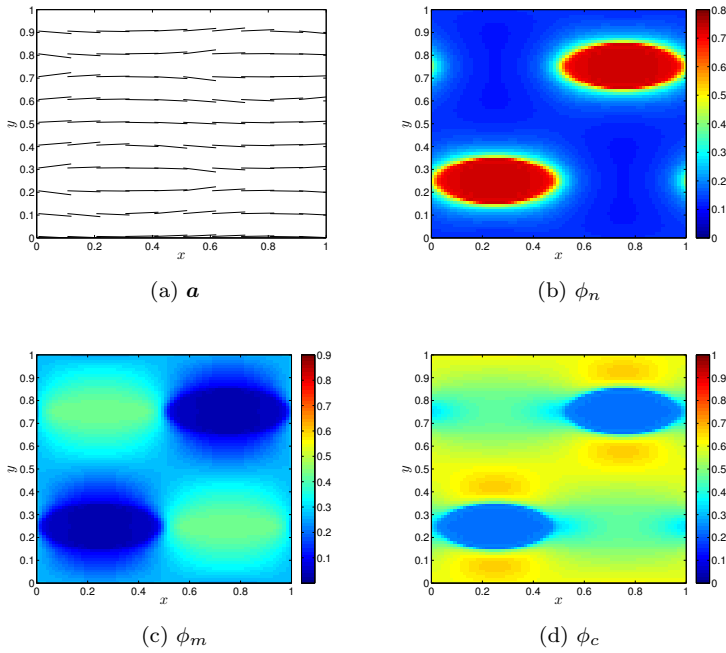


Fig. 12: Simulation results at time $t = 5.5$ with high shear viscosity in the fibre direction ($\mu_3 = 10$): (a) fibre alignment, \mathbf{a} ; (b) cell volume fraction, ϕ_n ; (c) medium volume fraction, ϕ_m ; (d) collagen volume fraction, ϕ_c . All other parameters and initial conditions as in Table 1.

spatial gradients in the cell and collagen densities and the divergence of the fibre director field.

The complexity of the model equations, together with the fact that we must consider at least a two-dimensional geometry if the effects of anisotropy are to be investigated, limit the analytical progress that can be made. However, a linearised analysis for the case of sparsely seeded cells reduces our system of equations to an anisotropic, nonlinear diffusion equation. This analysis reveals that fibre orientation influences cell distribution through enhanced cell diffusion in the fibre direction. The enhanced diffusive effect is related to the increased strength of the forces exerted by the cells on the fibres; it does not require the inclusion of anisotropic drag effects, and is independent of the mechanical properties of the collagen.

For arbitrary cell seeding densities, however, the equations governing the model must be solved numerically. Our results in §4 clearly demonstrate the importance of the often-neglected mechanical interactions between cells and the ECM for pattern formation in tissues. Changes to the initial fibre orientation in the collagen gel, the relative importance of the cell force term versus the affinity for the close-packing density, and the anisotropic mechanical prop-

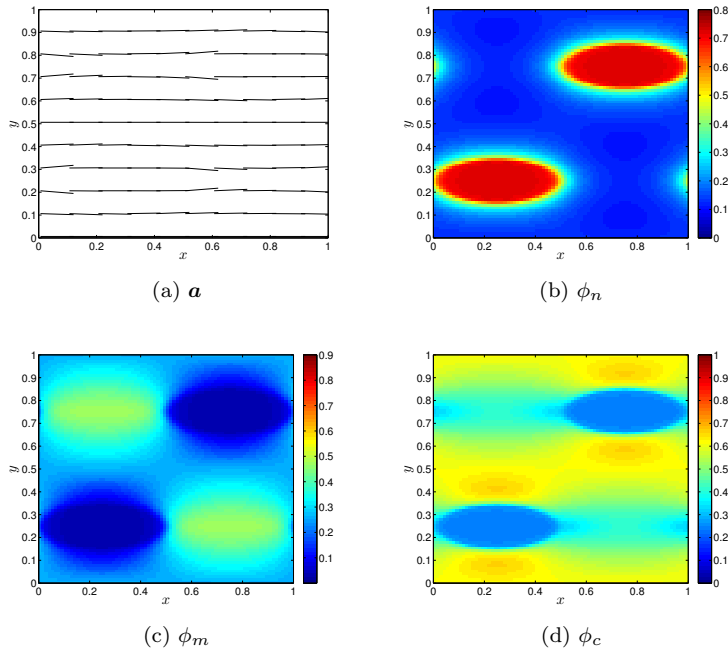


Fig. 13: Simulation results at time $t = 5.5$ with high fibre tension, extensional and shear viscosity in the fibre direction ($\mu_1 = \mu_2 = \mu_3 = 10$): (a) fibre alignment, \mathbf{a} ; (b) cell volume fraction, ϕ_n ; (c) medium volume fraction, ϕ_m ; (d) collagen volume fraction, ϕ_c . All other parameters and initial conditions as in Table 1.

erties of the collagen appear to have the greatest influence (at least over the parameter ranges we studied), resulting in changes to both the shape and orientation of the cell aggregates produced. The distribution of the collagen and medium, and the orientation of the fibres were also strongly affected. Thus the research presented here demonstrates the importance of these mechanisms in pattern formation, serving as a “proof of principle” that behaviour qualitatively similar to that seen in numerous biological systems can be generated in this way. However, further experimental and theoretical work will need to be undertaken before our model can be specialised to particular biological systems and used to make quantitative predictions. In particular, the mechanics of anisotropic materials such as collagen will need to be much better understood. For the simple transversely isotropic viscous fluid model used here, we need to know six parameters (μ_c^* , κ_c^* and μ_i^* for $i = 1, \dots, 4$), but at present an experimental protocol for measuring them has still to be developed. In addition, for simplicity we have neglected the influence of cell proliferation and chemical factors, although they play an important role in many tissue development and regeneration processes. For example, in vasculogenesis and

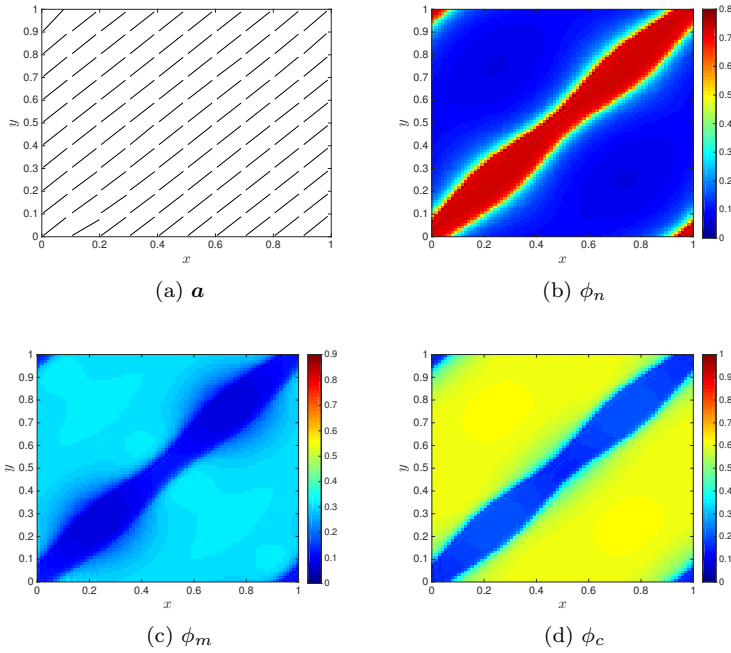


Fig. 14: Simulation results at time $t = 5$ with diagonal initial fibre alignment (given by 27) and high fibre tension, extensional and shear viscosity in the fibre direction ($\mu_1 = \mu_2 = \mu_3 = 10$): (a) fibre alignment, \mathbf{a} ; (b) cell volume fraction, ϕ_n ; (c) medium volume fraction, ϕ_m ; (d) collagen volume fraction, ϕ_c . All other parameters and initial conditions as in Table 1.

angiogenesis there is evidence that endothelial cells respond chemotactically to vascular endothelial growth factor, as outlined in Tosin et al (2006). The interaction of chemical and mechanical cues can therefore play a key role in tissue development and remodelling. Our multiphase modelling framework provides a solid basis for investigating these issues in future work.

Acknowledgements

We thank A.M. Soto and C. Sonnenschein (Tufts University) for the initial discussions which led to the development of the model, and D.J. Smith (University of Birmingham) for assistance with aspects of the numerics. RJD gratefully acknowledges the support of the University of Birmingham's System Science for Health initiative and the hospitality of the School of Mathematical Sciences at the University of Adelaide. JEF is supported by a Discovery Early Career Researcher Award (DE130100031) from the Australian Research Council. The work of HMB was supported in part by award KUK-C1-013-04, made by King Abdullah University of Science and Technology (KAUST).

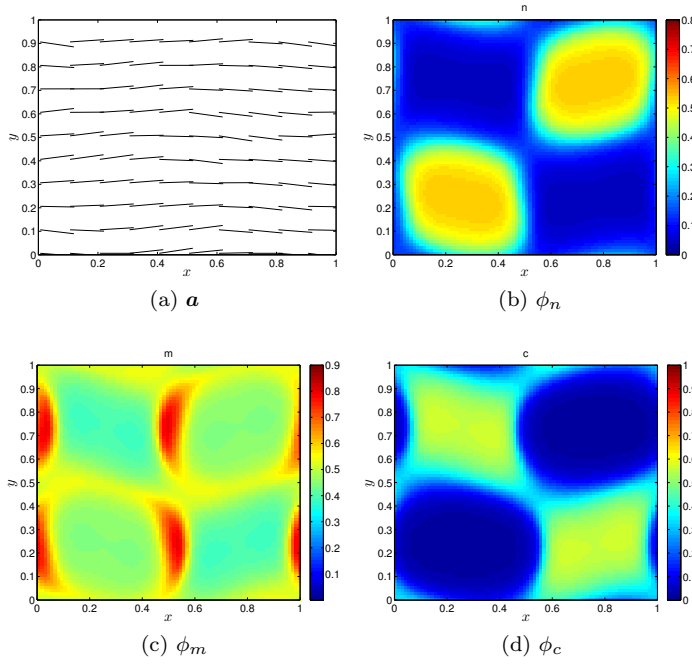


Fig. 15: Simulation results at time $t = 21$ with initial conditions and parameters as specified in (29, 30): (a) fibre alignment, \mathbf{a} ; (b) cell volume fraction, ϕ_n ; (c) medium volume fraction, ϕ_m ; (d) collagen volume fraction, ϕ_c . All other parameters and initial conditions as in Table 1.

A Approximation of the cell force, \mathbf{F}_c

In this Appendix, we give details of the calculation that leads to the leading-order expression for the cell force given in equation (14). Note that we suppress time dependence within this section for notational convenience. We begin by using the fact that $\mathbf{x}' = \mathbf{x} + \eta\boldsymbol{\xi}$, where $\eta \ll 1$, to expand the terms in equation (13) which are evaluated at \mathbf{x}' as follows:

$$\mathbf{a}(\mathbf{x}') = \mathbf{a}(\mathbf{x}) + \eta(\boldsymbol{\xi} \cdot \nabla)\mathbf{a}|_{\mathbf{x}} + O(\eta^2), \quad (31a)$$

$$\phi_n(\mathbf{x}') = \phi_n(\mathbf{x}) + \eta(\boldsymbol{\xi} \cdot \nabla)\phi_n|_{\mathbf{x}} + O(\eta^2), \quad (31b)$$

$$\phi_c(\mathbf{x}') = \phi_c(\mathbf{x}) + \eta(\boldsymbol{\xi} \cdot \nabla)\phi_c|_{\mathbf{x}} + O(\eta^2), \quad (31c)$$

where the notation $(\boldsymbol{\xi} \cdot \nabla)\mathbf{a}|_{\mathbf{x}}$ is intended to emphasise the fact that the directional derivatives are evaluated at the point \mathbf{x} .

On integration, the contribution of the leading-order terms in the integral is zero by symmetry. Proceeding to next order, we find

$$\begin{aligned} \mathbf{F}_c(\mathbf{x}) = \eta^{N+2} \int_{\Omega} F(|\boldsymbol{\xi}|)\boldsymbol{\xi} \left[\phi_c^2 \left(2\phi_n(\mathbf{a} \cdot \hat{\boldsymbol{\xi}})[(\boldsymbol{\xi} \cdot \nabla)\mathbf{a}] \cdot \hat{\boldsymbol{\xi}} \right. \right. \\ \left. \left. + (\mathbf{a} \cdot \hat{\boldsymbol{\xi}})^2(\boldsymbol{\xi} \cdot \nabla)\phi_n \right) + 2\phi_n\phi_c(\mathbf{a} \cdot \hat{\boldsymbol{\xi}})^2(\boldsymbol{\xi} \cdot \nabla)\phi_c \right] d^N\xi, \quad (32) \end{aligned}$$

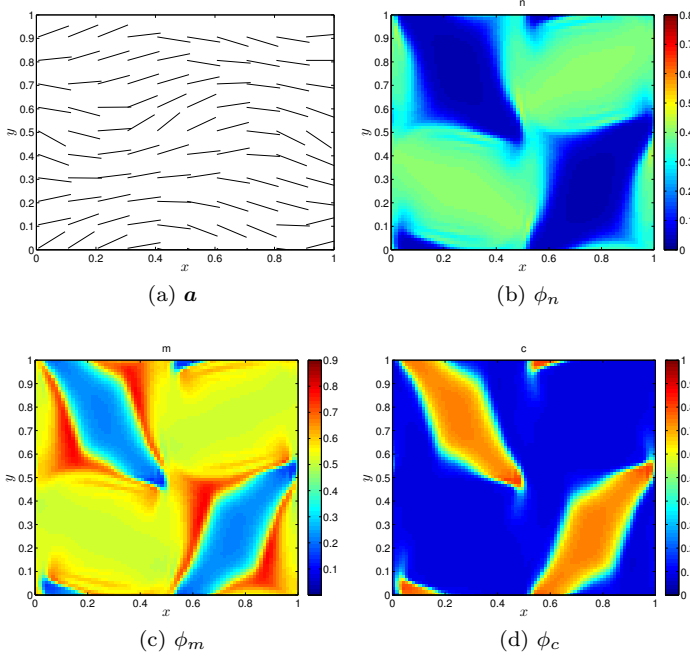


Fig. 16: Simulation results at time $t = 22$ with high anisotropic drag $d_{cn} = 100$ and initial conditions and parameters as specified in (29, 30): (a) fibre alignment, \mathbf{a} ; (b) cell volume fraction, ϕ_n ; (c) medium volume fraction, ϕ_m ; (d) collagen volume fraction, ϕ_c . All other parameters and initial conditions as in Table 1.

where $\hat{\boldsymbol{\xi}} = \boldsymbol{\xi}/|\boldsymbol{\xi}|$, and ϕ_n , ϕ_c and \mathbf{a} are evaluated at \mathbf{x} (unless otherwise stated). In component form we have

$$F_{c_i} = \eta^{N+2} \int_{\Omega} F(|\boldsymbol{\xi}|) \xi_i \left[\phi_c^2 \left(2\phi_n a_l \hat{\xi}_l \xi_k \frac{\partial a_j}{\partial x_k} \hat{\xi}_j + a_j \hat{\xi}_j a_l \hat{\xi}_l \xi_k \frac{\partial \phi_n}{\partial x_k} \right) + 2\phi_n \phi_c a_l \hat{\xi}_l a_j \hat{\xi}_j \xi_k \frac{\partial \phi_c}{\partial x_k} \right] d^N \boldsymbol{\xi}, \quad (33)$$

or, equivalently

$$F_{c_i} = \eta^{N+2} \int_{\Omega} F(|\boldsymbol{\xi}|) \frac{1}{|\boldsymbol{\xi}|^2} \xi_i \xi_j \xi_k \xi_l T_{ijkl} d^N \boldsymbol{\xi} = A_{ijkl}(\boldsymbol{\xi}) T_{ijkl}(\mathbf{x}), \quad (34)$$

where T_{ijkl} is independent of $\boldsymbol{\xi}$, and is given by

$$T_{ijkl}(\mathbf{x}) = \left(a_j \frac{\partial}{\partial x_k} (\phi_n \phi_c^2) + 2\phi_n \phi_c^2 \frac{\partial a_j}{\partial x_k} \right) a_l, \quad (35)$$

and

$$A_{ijkl} = \int_{\Omega} F(|\boldsymbol{\xi}|) \frac{1}{|\boldsymbol{\xi}|^2} \xi_i \xi_j \xi_k \xi_l d^N \boldsymbol{\xi}. \quad (36)$$

Since A_{ijkl} is an isotropic integral, it must be of the form (Spain, 1953)

$$A_{ijkl} = \lambda_1 \delta_{ij} \delta_{kl} + \lambda_2 \delta_{ik} \delta_{jl} + \lambda_3 \delta_{il} \delta_{jk}. \quad (37)$$

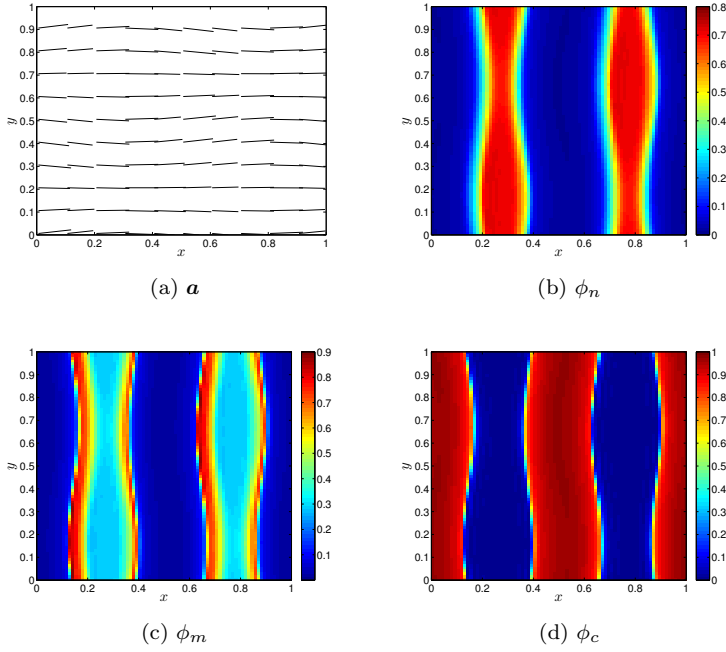


Fig. 17: Simulation results at time $t = 1.2$ with anisotropic drag ($d_{cn} = d_{cm} = 1$), high fibre tension ($\mu_1 = 10$) and a spatially varying initial fibre direction (28): (a) fibre alignment, \mathbf{a} ; (b) cell volume fraction, ϕ_n ; (c) medium volume fraction, ϕ_m ; (d) collagen volume fraction, ϕ_c . All other parameters and initial conditions as in Table 1.

Furthermore, since $A_{ijkl} = A_{ikjl} = A_{iljk}$, we deduce that

$$\lambda_1 = \lambda_2 = \lambda_3 = \lambda^*. \quad (38)$$

From equation (36) and (37) we note that

$$A_{iikl} = \int_{\Omega} F(|\xi|) \xi_k \xi_l d^N \xi = (N+2) \lambda^* \delta_{kl}, \quad (39)$$

and contracting over the remaining indices we obtain

$$N(N+2)\lambda^* = \int_{\Omega} F(|\xi|) |\xi|^2 d^N \xi. \quad (40)$$

Hence, on substituting equation (37) into equation (34), and on using the well-known properties of the Kronecker delta and the fact $|\mathbf{a}| = 1$, we find

$$\begin{aligned} \mathbf{F}_c(\mathbf{x}) = & \lambda [2\phi_n \phi_c^2 (\mathbf{a} \cdot \nabla) \mathbf{a} + \mathbf{a} \phi_c^2 (\mathbf{a} \cdot \nabla) \phi_n + \phi_n \mathbf{a} ((\mathbf{a} \cdot \nabla) \phi_c^2)] \\ & + \lambda [\phi_c^2 \nabla \phi_n + \phi_n \nabla (\phi_c^2)] + \lambda [2\phi_n \phi_c^2 (\nabla \cdot \mathbf{a}) \mathbf{a} + \phi_c^2 \mathbf{a} (\mathbf{a} \cdot \nabla) \phi_n + \phi_n \mathbf{a} (\mathbf{a} \cdot \nabla) \phi_c^2], \end{aligned} \quad (41)$$

where we have assumed that $\lambda = \eta^{N+2} \lambda^* = O(1)$. A little algebra then yields

$$\mathbf{F}_c(\mathbf{x}) = 2\lambda \left[(\mathbf{a} \cdot \nabla) (\phi_n \phi_c^2 \mathbf{a}) + \phi_n \phi_c^2 \mathbf{a} (\nabla \cdot \mathbf{a}) + \frac{1}{2} \nabla (\phi_c^2 \phi_n) \right]. \quad (42)$$

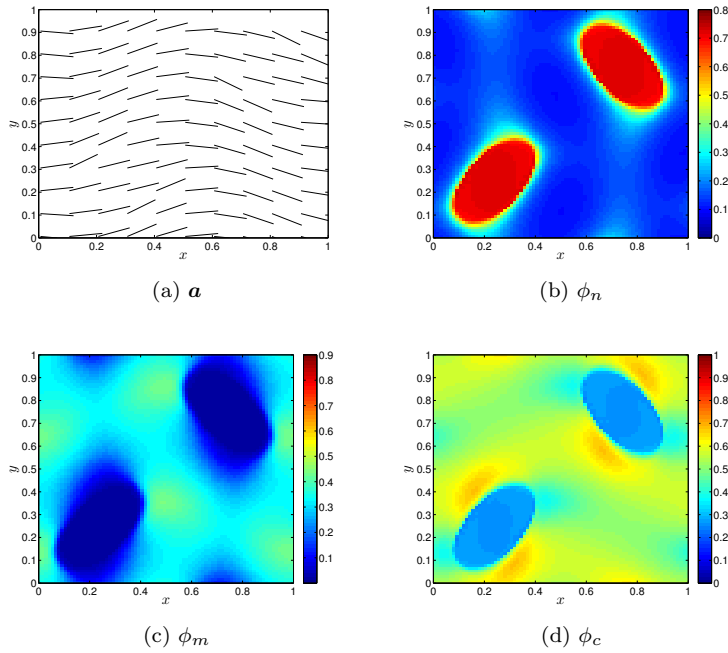


Fig. 18: Simulation results at time $t = 5.5$ with anisotropic drag ($d_{cn} = d_{cm} = 1$), small fibre tension ($\mu_1 = 0.1$), high extensional and shear viscosity in the fibre direction $\mu_2 = \mu_3 = 10$ and a spatially varying initial fibre direction (28): (a) fibre alignment, \mathbf{a} ; (b) cell volume fraction, ϕ_n ; (c) medium volume fraction, ϕ_m ; (d) collagen volume fraction, ϕ_c . All other parameters and initial conditions as in Table 1.

References

- Barocas VH, Tranquillo RT (1997) An anisotropic biphasic theory of tissue-equivalent mechanics: The interplay among cell traction, fibrillar network deformation, fibril alignment and cell contact guidance. *J Biomech Eng* 119:137 – 145
- Barocas VH, Moon AG, Tranquillo RT (1995) The fibroblast-populated collagen microsphere assay of cell traction force - Part 2: Measurement of the cell traction parameter. *J Biomech Eng* 117:p161–170
- Bissell MJ, Radisky D (2001) Putting tumours in context. *Nature Reviews Cancer* 1:46–54
- Breward CJW, Byrne HM, Lewis CE (2002) The role of cell-cell interactions in a two-phase model for avascular tumour growth. *J Math Biol* 45 (2):125–152
- Byfield FJ, Reen RK, Shentu TP, Levitan I, Gooch KJ (2009) Endothelial actin and cell stiffness is modulated by substrate stiffness in 2D and 3D. *J Biomech* 42(8):1114–1119
- Byrne HM, Preziosi L (2003) Modelling solid tumour growth using the theory of mixtures. *Math Med Biol* 20:341–366
- Byrne HM, King JR, McElwain DLS, Preziosi L (2003) A two-phase model of solid tumour growth. *Appl Math Lett* 16(4):567–573
- Chauviere A, Hillen T, Preziosi L (2007) Modelling cell movement in anisotropic and heterogeneous network tissues. *Networks and Heterogeneous media* 2(2):333–357

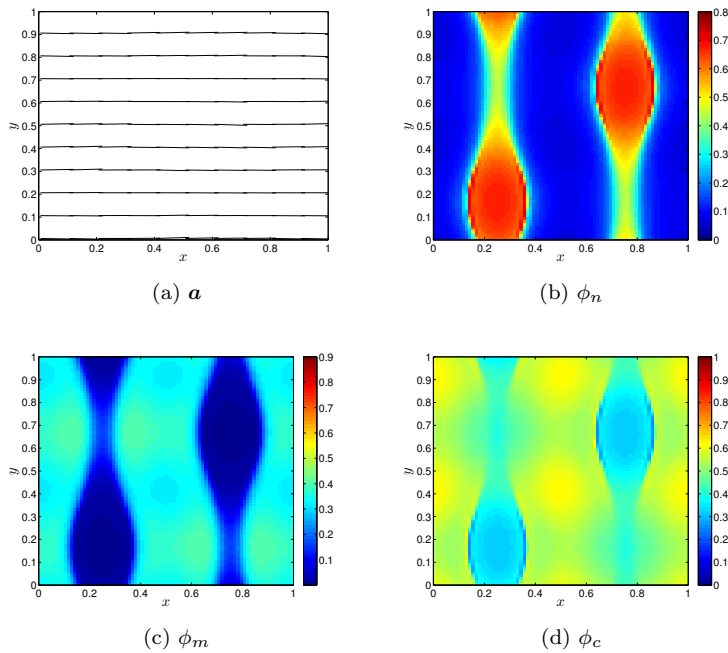


Fig. 19: Simulation results at time $t = 5.0$ with anisotropic drag ($d_{cn}, d_{cm} = 1$), high fibre tension, extensional and shear viscosity in the fibre direction $\mu_1 = \mu_2 = \mu_3 = 10$ and a spatially varying initial fibre direction (28): (a) fibre alignment, \mathbf{a} ; (b) cell volume fraction, ϕ_n ; (c) medium volume fraction, ϕ_m ; (d) collagen volume fraction, ϕ_c . All other parameters and initial conditions as in Table 1.

- Cockburn B, Shu CW (1998) The Runge–Kutta discontinuous Galerkin method for conservation laws. V *Journal of Computational Physics* 141:199–224
- Cook J (1995) Mathematical models for dermal wound healing: wound contraction and scar formation. PhD thesis, University of Washington
- Cukierman E, Bassi DE (2010) Physico-mechanical aspects of extracellular matrix influences on tumourigenic behaviours. *Seminars in Cancer Biology* 20(139–145)
- Dhimolea E, Maffini MV, Soto AM, Sonnenschein C (2010) The role of collagen reorganization on mammary epithelial morphogenesis in a 3d culture model. *Biomaterials* 31:3622–3630
- Drew DA (1983) Mathematical modelling of two-phase flow. *Ann Rev Fluid Mech* 15:261–291
- Dyson RJ, Jensen OE (2010) A fibre-reinforced fluid model of anisotropic plant cell growth. *J Fluid Mech* 655:472–503
- Engler AJ, Sen S, Sweeney HL, Discher DE (2006) Matrix elasticity directs stem cell lineage specification. *Cell* 126:677–689
- Ericksen JL (1960) Transversely isotropic fluids. *Colloid and Polymer Science* 173(2):117–122
- Eriksson K, Estep D, Hansbo P, Johnson C (1996) *Computational differential equations*. Cambridge University Press
- Gerisch A, Chaplain MAJ (2008) Mathematical modelling of cancer cell invasion of tissue: Local and non-local models and the effect of adhesion. *J Theor Biol* 250(4):684–704

- Green JEF, Friedman A (2008) The extensional flow of a thin sheet of incompressible, transversely isotropic fluid. *Euro J Appl Math* 19(3):p225–257
- Green JEF, Waters SL, Shakesheff KM, Byrne HM (2009) A mathematical model of liver cell aggregation *in vitro*. *Bull Math Biol* 71:906–930
- Green JEF, Waters SL, Shakesheff KM, Edelstein-Keshet L, Byrne HM (2010) Non-local models for the interactions of hepatocytes and stellate cells during aggregation. *J Theor Biol* 267(1):106–120
- Green JEF, Bassom AP, Friedman A (2013) A mathematical model for cell-induced gel compaction *in vitro*. *Math Model Meth Appl Sci* 23(1):127–163, DOI 10.1142/S0218202512500479
- Häcker A (2012) A mathematical model for mesenchymal and chemosensitive cell dynamics. *J Math Biol* 64:361–401
- Hillen T (2006) M^5 mesoscopic and macroscopic models for mesenchymal motion. *J Math Biol* 53(4):585–616
- Hinch EJ, Leal LG (1975) Constitutive equations in suspension mechanics. Part 1. General formulation. *J Fluid Mech* 71(3):481–495
- Hinch EJ, Leal LG (1976) Constitutive equations in suspension mechanics. Part 2. Approximate forms for a suspension of rigid particles affected by Brownian rotations. *J Fluid Mech* 76(1):187–208
- Holloway C, Dyson R, Smith D (2015) Linear taylor-couette stability of a transversely isotropic fluid. *Proc Roy Soc A* 471(2178), DOI 10.1098/rspa.2015.0141
- Ingber DE (2006) Mechanical control of tissue morphogenesis during embryological development. *Int J Dev Biol* 50:255–266
- Ingber DE (2008) Can cancer be reversed by engineering the tumour microenvironment? *Seminars in Cancer Biology* 18(5):356–364
- Jaalouk DE, Lammerding J (2009) Mechanotransduction gone awry. *Nature Reviews Molecular Cell Biology* 10:63–73
- Kabla A, Mahadevan L (2007) Nonlinear mechanics of soft fibre networks. *J R Soc Interface* 4(12):99–106
- Kirkpatrick ND, Andreou S, Hoying JB, Utzinger U (2007) Live imaging of collagen remodeling during angiogenesis. *Am J Physiol Heart Circ Physiol* 292(6):H3198–H3206
- Knapp DM, Barocas VH, Moon AG, Yoo K, Petzold LR, Tranquillo RT (1997) Rheology of reconstituted type I collagen gel in confined compression. *Journal of Rheology* 41:971–933
- Korff T, Augustin HG (1999) Tensional forces in fibrillar extracellular matrices control directional capillary sprouting. *J Cell Sci* 112:3249–3258
- Krause S, Maffini MV, Soto AM, Sonnenschein C (2008) A novel 3d *in vitro* culture model to study stromal-epithelial interactions in the mammary gland. *Tissue Eng* 14:261–271
- Kumar S, Weaver VM (2009) Mechanics, malignancy, and metastasis: The force journey of a tumour cell. *Cancer Metastasis Rev* 28:113–127
- Lee MEM (2001) Mathematical models of the carding process. PhD thesis, University of Oxford
- Lee MEM, Ockendon H (2005) A continuum model for entangled fibres. *Euro J Appl Math* 16:145–160
- Lemon G, King JR, Byrne HM, Jensen OE, Shakesheff KM (2006) Mathematical modelling of engineered tissue growth using a multiphase porous flow mixture theory. *J Math Biol* 52:571–594
- Lopez JI, Mouw JK, Weaver VM (2008) Biomechanical regulation of cell orientation and fate. *Oncogene* 27:6981–6993
- Manoussaki D, Lubkin S, Vernon R, Murray J (1996) A mechanical model for the formation of vascular networks *in vitro*. *Acta Biotheoretica* 44(3-4):271–282
- Martins-Green M, Bissell MJ (1995) Cell-ECM interactions in development. *Seminars in Developmental Biology* 6:149–159
- Murray JD (1993) *Mathematical Biology*, 2nd edn. Springer-Verlag, New York
- Namy P, Ohayon J, Tracqui P (2004) Critical conditions for pattern formation and *in vitro* tubulogenesis driven by cellular traction fields. *J Theor Biol* 227:103–120
- Nelson CM, Bissell MJ (2006) Of extracellular matrix, scaffolds, and signalling: Tissue architecture regulates development, homeostasis and cancer. *Ann Rev Cell Dev Biol* 22:287–309

- O'Dea RD, Waters SL, Byrne HM (2008) A two-fluid model for tissue growth within a dynamic flow environment. *Euro J Appl Math* 19(06):607–634
- O'Dea RD, Waters SL, Byrne HM (2010) A multiphase model for tissue construct growth in a perfusion bioreactor. *Math Med Biol* 27(2):95–127
- Olsen L, Maini PK, Sherratt JA, Dallon J (1999) Mathematical modelling of anisotropy in fibrous connective tissue. *Math Biosci* 158(2):145–170
- Osborne JM, Whiteley JP (2010) A numerical method for the multiphase viscous flow equations. *Computer Methods in Applied Mechanics and Engineering* 199:3402–3417
- Oster GF, Murray JD, Harris AK (1983) Mechanical aspects of mesenchymal morphogenesis. *J Embryol Exp Morph* 78:83–125
- Painter KJ (2009) Modelling cell migration strategies in the extracellular matrix. *J Math Biol* 58:511–543
- Petersen OW, Ronnov-Jessen L, Howlett AR, Bissell MJ (1992) Interaction with basement membrane serves to rapidly distinguish growth and differentiation pattern of normal and malignant human breast epithelial cells. *Proc Natl Acad Sci USA* 89(19):9064–9068, DOI 10.1073/pnas.89.19.9064
- Petrie CJS (1999) The rheology of fibre suspensions. *J Non-Newtonian Fluid Mech* 87:369–402
- Peyton SR, Ghajar CM, Khatiwala CB, Putnam AJ (2007) The emergence of ECM mechanics and cytoskeletal tension as important regulators of cell function. *Cell Biochem Biophys* 47:300–320
- Ronnov-Jessen L, Bissell MJ (2008) Breast cancer by proxy: can the microenvironment be both the cause and consequence? *Trends in molecular medicine* 15(1):5–13
- Schreiber DI, Barocas VH, Tranquillo RT (2003) Temporal variations in cell migration and traction during fibroblast-mediated gel compaction. *Biophys J* 84:4102–4114
- Soto AM, Sonnenschein C (2004) The somatic mutation theory of cancer: growing problems with the paradigm? *BioEssays* 26:1097–1107
- Spain B (1953) *Tensor Calculus*. Oliver and Boyd
- Stevenson MD, Sieminski AL, McLeod CM, Byfield FJ, Barocas VH, Gooch KJ (2010) Pericellular conditions regulate extent of cell-mediated compaction of collagen gels. *Biophys J* 99:19–28
- Strand DW, Franco OE, Basanta D, Anderson ARA, Hayward SW (2010) Perspectives on tissue interactions in development and disease. *Current Molecular Medicine* 10:95–112
- Szymanska Z, Morales-Rodrigo C, Lachowicz M, Chaplain MAJ (2009) Mathematical modelling of cancer invasion of tissue: the role and effect of nonlocal interactions. *Math Models Meth Appl Sci* 19(2):257–281
- Takakuda K, Miyairi H (1996) Tensile behaviour of fibroblasts cultured in collagen gel. *Biomaterials* 17(14):1393 – 1397
- Thompson DW (1942) *On Growth and Form*, 2nd edn. Cambridge University Press
- Tosin A, Ambrosi D, Preziosi L (2006) Mechanics and chemotaxis in the morphogenesis of vascular networks. *Bull Math Biol* 68(7):1819–1836
- Tranquillo RT, Murray JD (1993) Mechanistic model of wound contraction. *J Surg Res* 55:233–247
- Vader D, Kabla A, Weitz D, Mahadevan L (2009) Strain-induced alignment in collagen gels. *PLoS ONE* 4(6):e5902, DOI 10.1371/journal.pone.0005902
- Weigelt B, Bissell MJ (2008) Unravelling the microenvironmental influences on the normal mammary gland and breast cancer. *Seminars in Cancer Biology* 18:311–321
- Wipff PJ, Rifkin DB, Meister JJ, Hinz B (2007) Myofibroblast contraction activates latent TGF- β 1 from the extracellular matrix. *J Cell Biol* 179(6):1311–1323